European Journal of Medicinal Chemistry 78 (2014) 401–418

Contents lists available at ScienceDirect

European Journal of Medicinal Chemistry

journal homepage: http://www.elsevier.com/locate/ejmech

Original article

Design and synthesis of a hybrid series of potent and selective agonists of α7 nicotinic acetylcholine receptor

Arianna Nencini [a,*], Cristiana Castaldo [a], Thomas A. Comery [b], John Dunlop [b,1], Eva Genesio [a], Chiara Ghiron [a,2], Simon Haydar [b,3], Laura Maccari [a], Iolanda Micco [a], Elisa Turlizzi [a], Riccardo Zanaletti [a,4], Jean Zhang [b]

[a] Siena Biotech SpA, Strada del Petriccio e Belriguardo 35, 53100 Siena, Italy
[b] Neuroscience Research Unit, Pfizer, Eastern Point Road, Groton, CT 06340, United States

ARTICLE INFO

Article history:
Received 19 December 2013
Received in revised form
10 February 2014
Accepted 11 March 2014
Available online 19 March 2014

Keywords:
Neuronal nicotinic acetylcholine receptors
Nicotinic ligands
Cognition
Alzheimer's disease
Schizophrenia

ABSTRACT

α7 nicotinic acetylcholine receptor agonists are promising therapeutic candidates for the treatment of cognitive impairment. As a follow up of our internal medicinal chemistry program we investigated a novel series of α7 nAChR agonists. Starting from molecular docking studies on two series of molecules recently developed in our laboratories, an alternative scaffold was designed attempting to combine the optimal features of these previously identified urea and pyrazole compounds. Based on our previous SAR knowledge and on predicted drug-like properties, a small library was synthesized in parallel manner, affording compounds with excellent α7 nAChR activity, selectivity and preliminary ADME profile.

© 2014 Elsevier Masson SAS. All rights reserved.

1. Introduction

Neuronal nicotinic acetylcholine receptors (nAChRs) are a family of ligand gated ion channels that are distributed both in the central and peripheral nervous system and are permeable to cations such as Na^+, K^+ and Ca^{2+} [1–3]. These receptors play an important role in different physiological processes and alterations in their number and/or function are associated with several pathologies. The homomeric α7 nAChR is one of the most abundant nicotinic receptors in the human brain and is highly expressed in the cerebral cortex and the hippocampus, regions that are associated with memory and learning [4]. The involvement of α7 nAChR in pathologies such as Alzheimer's disease (AD) and schizophrenia has been supported by different research studies [5,6]. For example, expression of α7 nAChR was found to be reduced in the brain tissues of both AD and schizophrenia patients [7]. Prototypical α7 receptor agonists have demonstrated to improve cognition in animal models and normalize sensory gating deficits, which are believed to contribute to the cognitive fragmentation in schizophrenia [8,9]. In accordance to this hypothesis, the prototypical nAChR agonist nicotine, as well as more selective α7 agonists recently described, have been shown to improve cognitive performance in both animal models and human clinical trials [10,11]. In the past decade, there has been a continuous effort to develop new α7 nAChR agonists with better properties, focusing mainly on two different types of compounds: full agonists and partial agonists [12]. Although it may be speculated that the level of agonist efficacy and/or potency plays a role in driving certain physiological and

Abbreviations: ACh, acetylcholine; AChBP, acetylcholine binding protein; AD, Alzheimer's disease; ADME, absorption, distribution, metabolism, and excretion; ACN, acetonitrile; B/P, brain to plasma ratio; CDI, 1,1′-carbonyldiimidazole; DCM, dichoromethane; DMAP, 4-N,N-dimethylaminopyridine; ESI, electrospray ionization; FLIPR, fluorescence imaging plate reader; HBD, hydrogen bond donor; HBSS, Hank's balanced salt solution; HEK, human embryo kidney; HPLC, high pressure liquid chromatography; LTQ, linear trap quadrupole; MDCK, Madin Darby canine kidney; MFC, 7-Methoxy-4-trifluoromethylcoumarin; MPSA, molecular polar surface area; MS, mass spectrometry; nAChR, nicotinic acetylcholine receptor; P450, cytochrome P450; PAMPA, parallel artificial membrane permeability assay; PDA, photodiode array; Rt, retention time; SAR, structure–activity relationship; TBTU, O-(Benzotriazol-1-yl)-N,N,N′,N′-tetramethyluronium tetrafluoroborate; THF, tetrahydrofuran; TLC, thin layer chromatography; TOF, time-of-flight; TPSA, topological polar surface area; UPLC, ultra performance liquid chromatography.

* Corresponding author.
E-mail addresses: anencini@sienabiotech.it, arianna.nencini@gmail.com (A. Nencini).
[1] Neuroscience Innovative Medicines Unit, AstraZeneca, 141 Portland Street, Cambridge, MA 02139, United States.
[2] Strada Comunale di Salteano 1, Isola d'Arbia, 53041 Siena, Italy.
[3] Eli Lilly and Company, Indianapolis, IN 46285, USA.
[4] Aptuit Srl., Via Alessandro Fleming 4, 37135 Verona (VR), Italy.

http://dx.doi.org/10.1016/j.ejmech.2014.03.031
0223-5234/© 2014 Elsevier Masson SAS. All rights reserved.

cognitive functions, studies with very weak partial agonists, partial agonists and full agonists show that *in vivo* efficacy can be realized by ligands belonging to these profiles [13]. In addition, either full or partial agonists entered the clinical trials and in most cases no adverse effects ascribed to the α7 agonism on peripheral tissues were reported [12]. An alternative approach to target α7 nAChR is the use of positive allosteric modulators (PAMs), which enhance the effect elicited by the endogenous ligand without directly activating or desensitizing the target receptor [14].

Our research group focused on the identification of α7 nAChR full agonists and we formerly disclosed important series of compounds [15–17], characterized by the presence of a terminal basic amine, a linear spacer, a linker (urea or amide) and an aromatic region (Fig. 1).

The most advanced molecules of these series are depicted in Table 1: SEN34625/WYE-103914 (**1**) has overall good properties and excellent pharmacokinetic profile but maintains an antagonist effect on α3 (7.3 μM) and α1 (15.1 μM) containing nicotinic receptors, a common issue of all the urea series. On the other hand the most representative compound of the pyrazole series, SEN78702/WYE-308775 (**2**) shows complete selectivity against the three homologous receptors and good pharmacokinetic properties but has lower potency at the α7 receptor.

A homology model for the human α7 receptor has been previously described [16] which has been able to predict the binding mode for our series of analogues consistently with their SAR. In particular, docking studies identified the basic centre as an anchoring point engaged in a hydrogen bond with the backbone carbonyl of W143; the urea linker and the amide-pyrazole moiety in the two previously reported series respectively provide a double H-bonding system to Y185; this part of the molecule also stacks over Y89. The alkyl chain acts as spacer between these two pharmacophoric features and demonstrated to play a significant role in modulating receptor activity.

In the present paper we describe our efforts in the identification of a new back-up series, designed to combine the best features of the urea series (potency on α7 nAChR) and the pyrazole series (selectivity on α1 and α3 containing nicotinic and 5HT3 receptors). To achieve this goal we focused our work on the rational design of new series of compounds, mainly modifying the linear spacer, a portion of the molecule that was scarcely explored in our previous activities.

2. Chemistry

The compounds required for SAR exploration were prepared following four different synthetic routes. Route A was followed to

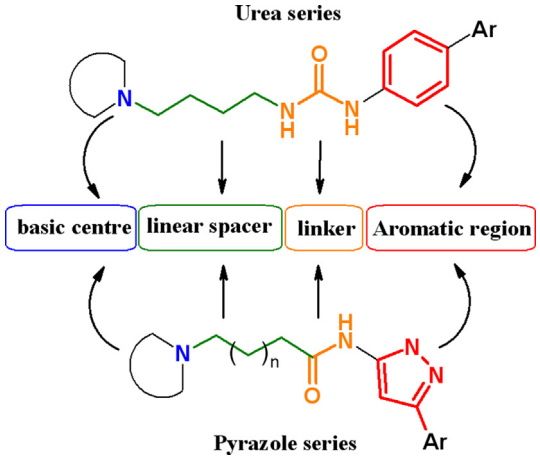

Fig. 1. General structure of most advanced series of α7 nAChR agonists.

Table 1
Activity and selectivity profile of most advanced compounds of urea and pyrazole series.

Compound	Activity EC_{50} (μM) α7	Selectivity IC_{50} (μM) α1	α3	$5HT_3$
1 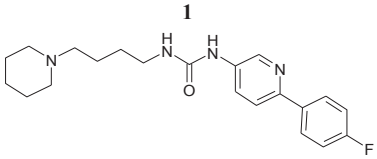	0.07	15.1	7.3	>30
2 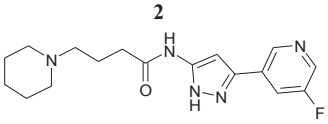	0.90	>30	>30	>30

prepare compounds with a linear carbon chain, as we previously described [15]; it consists of four synthetic steps (Scheme 1): alkylation of 4-bromo-butylphthalimide (**3**) with piperidine, to give intermediate **4**, which was then deprotected in the presence of hydrazine to yield compound **5**. Reaction of amine **5** with 4-bromophenylisocyanate afforded urea **6**, which underwent Suzuki–Miyaura coupling with the desired boronic acid to obtain the final compounds **7**.

Route B was used for compounds with a cyclic carbon chain and is reported in Scheme 2.

Key intermediates of this synthetic approach were amines **14a–d**. Amine **14a** was commercially available. Amines **14b** and **14c** were prepared in three steps: N-boc-isonipecotic acid (**8a**) or N-boc-nipecotic acid (**8b**) were coupled to piperidine (in the presence of TBTU as coupling agent) obtaining the corresponding amides **9a** and **9b**, which were deprotected with 6 N hydrochloric acid at room temperature and finally reduced with $LiAlH_4$ affording intermediates **14b** and **14c**. Amine **14d** was prepared in three steps: commercially available 4-(2-hydroxy-ethyl)-piperidine-1-carboxylic acid tert-butyl ester (**11**) was activated with tosyl chloride and 4-N,N-dimethylaminopyridine (DMAP) giving the corresponding tosylate **12** which underwent a nucleophilic substitution with piperidine to afford intermediate **13**, which was then deprotected, with 6 N hydrochloric acid at room temperature to yield amine **14d**. Amines

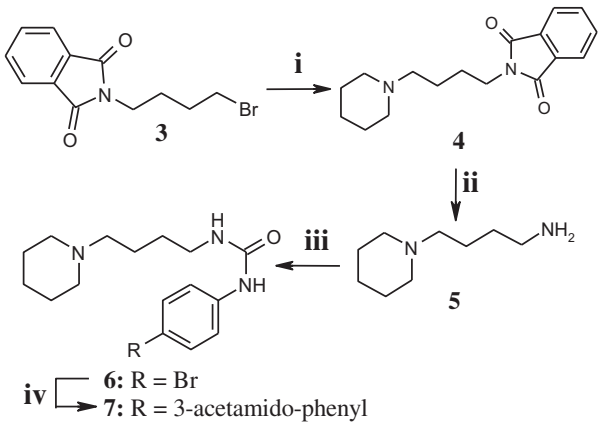

Scheme 1. Route A, reagents and conditions: (i) piperidine, butanol, 110 °C; (ii) hydrazine monohydrate, EtOH, 70 °C, 2 h; (iii) 4-bromophenylisocyanate, DCM; (iv) 3-acetamidophenyl boronic acid, $Pd(PPh_3)_4$, Na_2CO_3, ACN/H_2O.

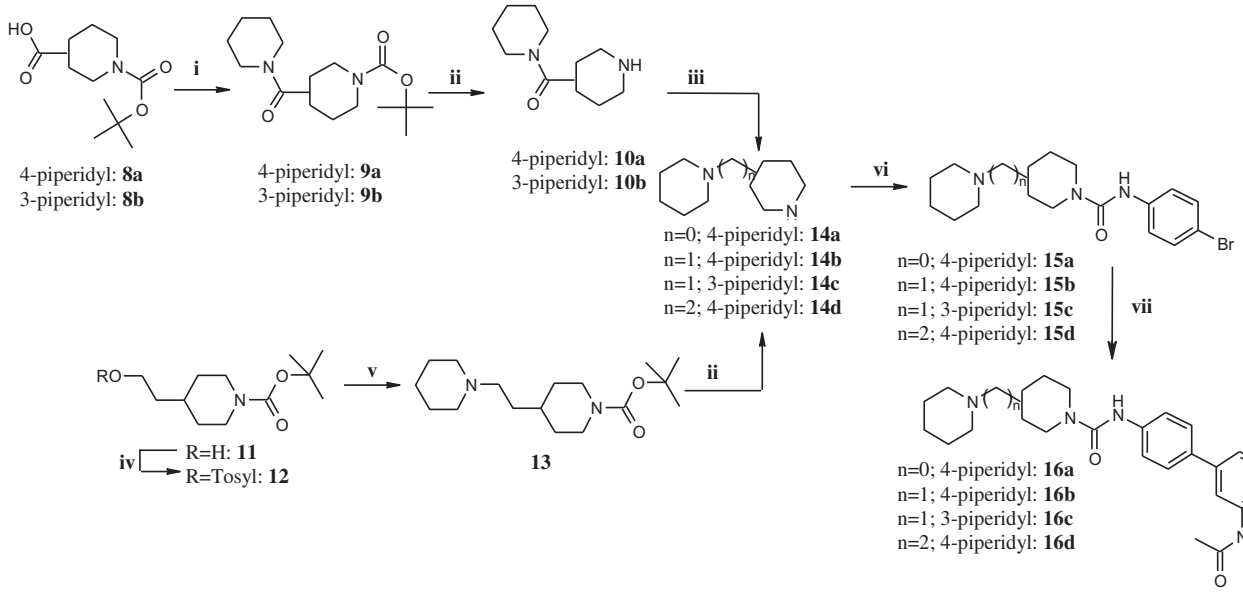

Scheme 2. Route B, reagents and conditions: (i) TBTU, piperidine; (ii) HCl 6 N, 0 °C to r.t.; (iii) $LiAlH_4$, THF, reflux; (iv) Tosyl chloride, DMAP, DCM; (v) piperidine, acetonitrile, reflux; (vi) 4-bromo-phenyl isocyanate, DCM, r.t.; (vii) $ArB(OH)_2$, P(o-tolyl)$_3$, Pd/C(10%), Na_2CO_3 dimethoxyethane/H_2O, microwave irradiation 90 °C.

14a–**d** were reacted with 4-bromophenylisocyanate to give the corresponding ureas (**15a**–**d**), and finally coupled to the selected boronic acid in a Suzuki–Miyaura reaction, affording the final compounds (**16a**–**d**). During this step we observed that using previously reported coupling conditions [15] the urea moiety of starting materials (**15a**–**d**) and of final compounds (**16a**–**d**) was quite prone to hydrolysis (Scheme 3), generating variable amounts of 4-bromoaniline (**16e**), biphenylaniline (**16f**) and the corresponding secondary amines (**14a**–**d**), with consequent difficulties during the purification and low final yields. After a careful screening of several solvent mixtures, bases and phosphines, we identified the optimal condition to have complete conversion and avoid hydrolysis: 1,2-dimethoxyetane/water (9:1) as solvent, 2 equivalents Na_2CO_3 as base and tri-*o*-tolylphosphine as palladium ligand.

Route C was used to prepare pyrazole derivatives with linear carbon chain and is illustrated in Scheme 4. As previously described [16,17], nucleophilic substitution on ω-bromoalkanoic esters (**17a** and **17b**) with piperidine or pyrrolidine afforded aminoesters **18a**–**c**, which were then hydrolyzed in the presence of NaOH to the corresponding acids **19a**–**c**. Finally, coupling of **19a**–**c** with the desired 3-amino-5-aryl pyrazoles (**20a**–**d**) afforded compounds **21a**–**h**. Amide reduction of compounds **21a** and **21b** with $LiAlH_4$ in THF at reflux, gave compounds **22a** and **22b**.

Route D was followed for pyrazole derivatives with cyclic carbon chain and is depicted in Scheme 5. Selective ring N-protection [18] of aminopyrazoles **20a**–**d** gave the corresponding *tert*-butylcarbamates (**23a**–**d**); following a reported literature procedure [19], compounds **23a**–**d** were converted in the corresponding isopropenyl carbamates **24a**–**d**. Intermediates **24a**–**d** were reacted in parallel with commercially available amines **25a**–**d**, obtaining the corresponding unsymmetrical ureas **26a**–**p** with complete N-pyrazole deprotection in a single step; compounds **27a**–**d** derive from nucleophilic attack of the secondary amines **25a**–**d** on the pyrazole *tert*-buyl carbamate and could be easily removed from the desired products using chromatographic methods.

3-Amino-5-aryl pyrazole **20a** was found to be commercially available, while **20b**–**d** were synthesized according to literature procedures [20–22], as depicted in Scheme 6. Acid **28b**–**d** were converted to the corresponding methyl esters (**29b**–**d**), refluxing in methanol in the presence of a catalytic amount of sulfuric acid;

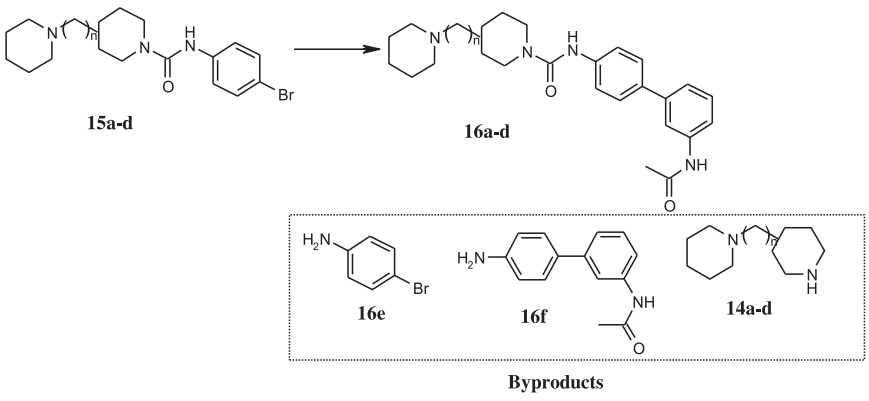

Scheme 3. Byproducts of Suzuki coupling.

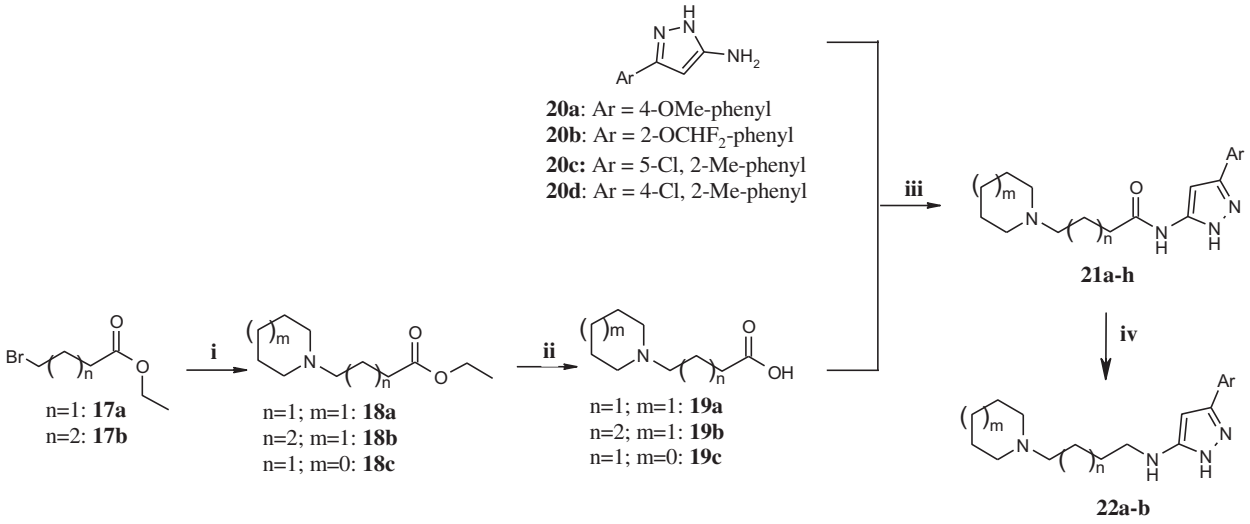

Scheme 4. Route C reagents and conditions: (i) piperidine, toluene, reflux; (ii) NaOH, water, reflux; (iii) CDI, 1,2-dichloroethane, 50 °C; (iv) $LiAlH_4$, THF reflux.

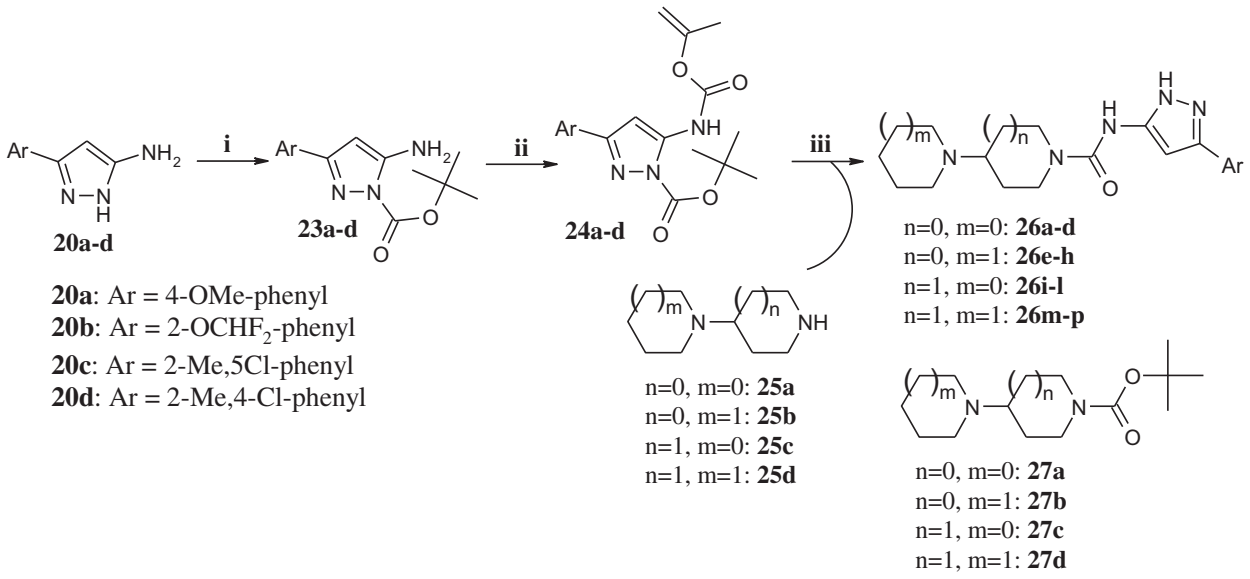

Scheme 5. Route D reagents and conditions: (i) KOH, DCM/H_2O; (ii) isopropenyl chloroformate, triethylamine, DCM, r.t.; (iii) 4-aryl aminopyrazole, THF reflux.

esters **29b**–**d** were reacted with *in situ* generated acetonitrile anion to give β-ketonitriles **30b**–**d**, which underwent nucleophilic attack of hydrazine, affording aminopyrazoles **20b**–**d**.

3. NMR experiments

For most of the compounds bearing a pyrazole system (amides **21a**–**h**, amines **22a**–**b** and ureas **26a**–**p**), ^{13}C NMR spectra were not completely resolved using DMSO-d6 as solvent and running the experiments at room temperature. The ^{13}C signals of the aminopyrazole core tend to be very broad [23] due to the tautomeric equilibrium exchange that is slow on the NMR timescale (Fig. 2). To improve the signal to noise ratio of these specific signals the polarity of the NMR solvent was changed (from DMSO-d6 to CD_3OD or adding formic acid to free bases DMSO solutions). In case of poor solubility, the experimental temperature (VT) was raised up to 80 °C to enhance the exchange rate between the two tautomeric forms. See experimental section and Supplementary Data for more details.

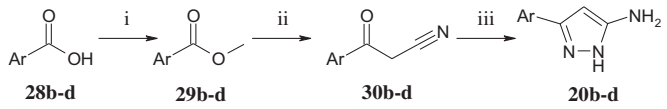

Scheme 6. Synthesis of 3-amino-5-aryl pyrazole – Reagents and conditions: (i) H_2SO_4, MeOH reflux; (ii) ACN, BuLi, toluene −78 °C to rt; (iii) Hydrazine monohydrate, ethanol reflux.

4. Pharmacology

The activity and selectivity profile of synthesized compounds **7**, **16a**–**d**, **21a**–**h**, **22a**–**b** and **26a**–**p** were measured in a calcium flux assay using a fluorescence imaging plate reader [24]. Activity at rat

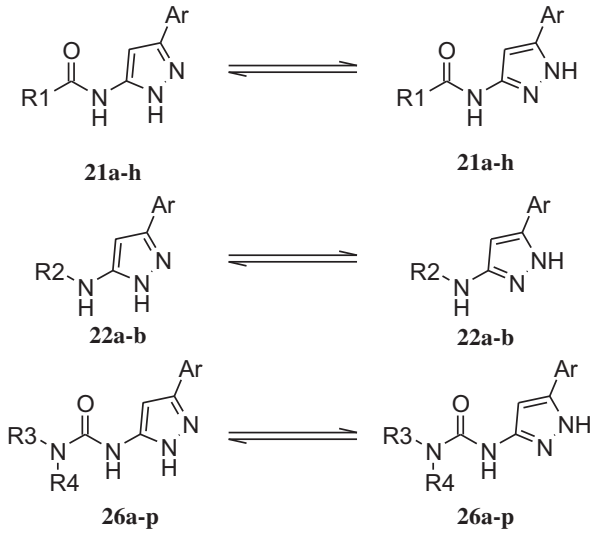

Fig. 2. Tautomeric equilibrium of pyrazole derivatives.

α7-nAChRs was determined using a stable recombinant GH4C1 cell line transfected with pCEP4/rat α7 nAChR as previously described [24]. To verify whether the changes in Ca^{+2} levels were specifically due to nAChR opening, we developed a counter screen on GH4C1 wild type cells. Compounds with E_{max} >70% of nicotine were considered to be full agonists. Reported EC_{50}/IC_{50} values were obtained from triplicate data points. Nicotine under the same conditions had EC_{50} = 1.34μM ± 0.002, E_{max} = 102% ± 1.3 (n = 62), Acetylcholine EC_{50} = 3.12μM ± 0.13, E_{max} = 110% ± 4.1 (n = 6), PHA568,487 EC_{50} = 0.037μM ± 0.002, E_{max} = 94% ± 4.5 (n = 2). Even if literature reports human and rat α7-nAChRs to be not pharmacologically identical [25], we have observed comparable EC_{50} values for these two different species when testing compounds belonging to the originating series [16,17]. For selectivity assessment against the 5HT3 receptor, HEK293 cell lines stably expressing human 5-HT3A receptors were used; while for α1 and α3 containing receptors TE671 rhabdomyosarcoma cells and neuroblastoma SH-SY5Y cells were respectively used [24]. Preliminary ADME profile consisted of the measurement of solubility (determined at pH 7.4 at pseudothermodynamic equilibrium), permeability (permeation rate of the test article through an artificial membrane) and metabolic stability (determined as percentage remaining after incubation for 1 h with recombinant hCYP3A4). All these data are reported in Tables 1–4. See Experimental Section for further details on all assays.

5. Results and discussion

The first attempt of designing a back-up series consisted of the replacement of the linear spacer of urea series with a cycle, in order to reduce the number of rotatable bonds and remove one hydrogen bond donor (HBD), to improve the drug likeness of the compounds [26,27] and observe the potential effect on the activity and selectivity profiles. We designed a small set of compounds (series A) whose activity and selectivity data are reported in Table 2 (while an overview of calculated properties including MW, clog*P*, TPSA, number of rotatable bond, number of HBD and logBB are reported in Table S1 of supplementary data). We started from compound **7**, a very potent analogue of **1**, which suffered from poor selectivity against the α-3 containing nicotinic receptor and low passive permeability. We replaced the linear carbon chain of **7** with piperidine (**16a**), 4-methyl-piperidine (**16b**), 3-methyl-piperidine (**16c**) and 4- ethyl-piperidine (**16d**). All these modifications caused a decrease of activity on α-7 receptor: **16a** and **16b** had more than 20 fold loss of activity, compound **16c** was completely inactive and

Table 2
Activity, Selectivity (EC_{50} for Agonist Behavior, IC_{50} for Antagonist Behavior), Solubility, Permeability (Perm Class), Metabolic Stability (Stability Class), of compounds of Series A compared to original urea series.

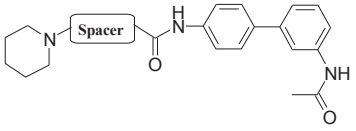

Compd	Spacer	Activity[a] EC_{50} μM (E_{max}) α7	Selectivity[a] IC_{50} (μM) α1	α3	$5HT_3$	Sol[b] (μM)	Perm[c]	Met stab[d]
7	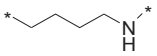	0.07 (133)	>30	1.16	>30	142	Low	91
16a	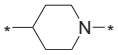	1.85 (106)	>30	>30	>30	202	Low	92
16b	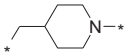	2.26 (124)	>30	>30	>30	162	High	95
16c	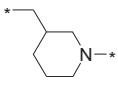	>30	NT	NT	NT	250	High	100
16d	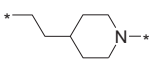	0.50 (128)	>30	>30	>30	250	High	90

[a] Reported EC_{50}/IC_{50} values were determined from triplicate data points; E_{max} is expressed as percentage of nicotine 10 μM signal. NT means not tested.
[b] Solubilities were determined at pH 7.4 at pseudothermodynamic equilibrium.
[c] Permeability is based on measuring the permeation rate of the test article through an artificial membrane. The assay uses a mixture of porcine pig brain lipids in dodecane (2% w/v).
[d] Metabolic stability was determined as percentage remaining after incubation for 1 h with recombinant hCYP3A4.

Table 3
Activity, Selectivity (EC_{50} for Agonist Behavior, IC_{50} for Antagonist Behavior), Solubility, Permeability (Perm Class), Metabolic Stability (Stability Class), for compounds of Series B.

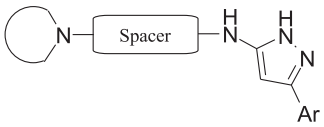

Compd	Amine	Spacer	Ar	Activity[a] EC_{50} μM (E_{max}) α7	Selectivity[a] IC_{50} (μM) α1	α3	5HT3	Sol[b] (μM)	Perm[c]	Met Stab[d]
21a		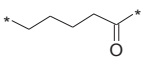	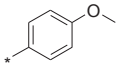	0.43 (106)	>30	3.30	>30	219	High	100
22a			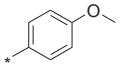	2.80 (73)	27.7	7.97	>30	198	High	100
21b		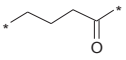	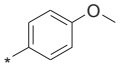	0.42 (121)	>30	16.8	>30	174	High	100
22b		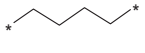	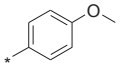	0.45 (104)	26.8	1.7	>30	206	High	100
21c		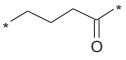	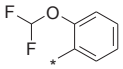	0.12 (105)	>30	>30	15.0	142	High	100
21d		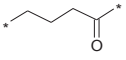	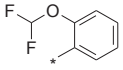	0.22 (114)	24.7	12.1	10.9	133	High	100
21e		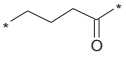	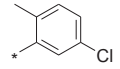	0.07 (118)	16.9	14.2	12.1	113	High	54
21f		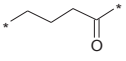	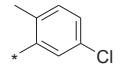	0.15 (103)	4.30	3.36	13.5	125	High	41
21g		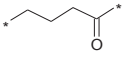	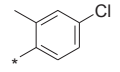	0.15 (129)	10.9	4.16	>30	113	High	83
21h		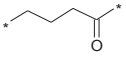	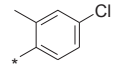	0.28 (90)	7.05	3.20	11.6	105	High	56

[a] Reported EC_{50}/IC_{50} values were determined from triplicate data points; E_{max} is expressed as percentage of nicotine 10 μM signal.
[b] Solubilities were determined at pH 7.4 at pseudothermodynamic equilibrium.
[c] Permeability is based on measuring the permeation rate of the test article through an artificial membrane. The assay uses a mixture of porcine pig brain lipids in dodecane (2% w/v).
[d] Metabolic stability was determined as percentage remaining after incubation for 1 h with recombinant hCYP3A4.

only **16d** had an EC_{50} value below 1 μM. From a docking perspective, these molecules suffer from the loss of one of the two hydrogen-bonding NH groups characterizing the urea or amide-pyrazole series, while the remaining one is made less accessible by the neighboring piperidine ring. Few docking poses show an alternative conformation where the amidic carbonyl group functions as a hydrogen bond acceptor for Y185. It appears that in all these compounds the double hydrogen-bonding interaction typically engaged by the urea or amide-pyrazole moieties is disrupted causing a general drop in activity. In the case of compound **16c**, the 3-piperidine ring forces the molecule into a different overall shape so that it cannot engage in the usual pharmacophoric interactions anymore. On the other hand, the selectivity profile was really encouraging as the activity on α3 containing nicotinic receptor was abolished and selectivity against α1 containing nicotinic and 5HT3 receptors was maintained. A preliminary ADME evaluation confirmed good properties for all the compounds. HBD removal from original urea **7**, generally increased passive permeability (with the only exception of **16a**) while good solubility and metabolic stability values were confirmed for all the analogues **16a**–**d**. In light of this quick SAR exploration we deduced that a cyclic spacer would be a good structural modification to improve selectivity of our molecules and modulate α7 activity. In the mean time we also tried to modify the original pyrazole series in order to obtain more potent compounds. Also in this case we started to work on the linear spacer (Table 3), by removing from representative

compounds **21a** and **21b** the carbonyl group, which is involved in the delocalization of the pi-system over the amide moiety and predicted by docking studies to contribute to the stacking interaction over Y89. Confirming this hypothesis, we observed that compound **22a** was 6 times less active then the analogue **21a** on α7, while **22b** maintained the same activity of **21b** but lost selectivity against the α3 containing nicotinic receptor. Another strategy to improve activity of Series B was the exploration of different basic amines and aromatic groups. Representative examples are reported in Table 3 (while an overview of calculated properties is reported in Table S2 of supplementary data). As we previously observed, with no exceptions, pyrrolidine derivatives showed lower EC_{50} values than piperidine bearing compounds in terms of activity on α7 and better selectivity profile against the three related receptors (for

Table 4
Activity, Selectivity (EC_{50} for Agonist Behavior, IC_{50} for Antagonist Behavior), Solubility, Permeability (Perm Class), Metabolic Stability (Stability Class), for compounds of Series C.

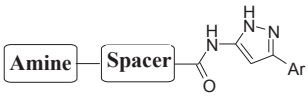

Compd	Amine	Spacer	Ar	Activity[a] EC_{50} μM (E_{max}) α7	Selectivity[a] IC_{50} (μM) α1	α3	5HT3	Sol[b] (μM)	Perm[c]	Met Stab[d]
26a		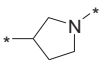	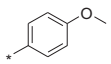	0.69 (93)	>30	>30	>30	126	High	100
26b		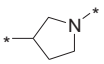	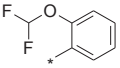	0.27 (96)	>30	>30	>30	123	High	99
26c		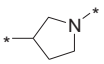	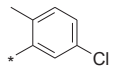	0.23 (88)	>30	>30	>30	97	High	64
26d		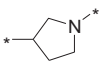	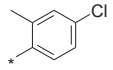	0.57 (77)	>30	>30	>30	99	High	54
26e		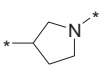	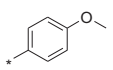	0.48 (75)	>30	>30	>30	118	High	93
26f		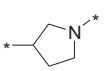	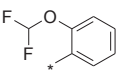	0.30 (81)	>30	>30	>30	111	High	55
26g		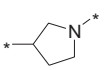	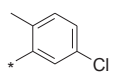	0.35 (88)	>30	>30	>30	84	High	47
26h		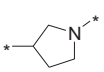	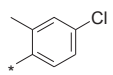	0.30 (73)	>30	>30	>30	70	High	47
26i		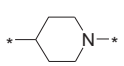	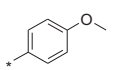	1.32 (97)	NT	NT	NT	151	High	100
26j		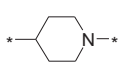	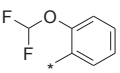	0.92 (90)	>30	>30	>30	129	High	100
26k		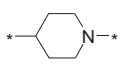	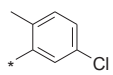	0.38 (76)	>30	>30	>30	121	High	93
26l		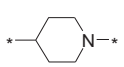	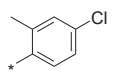	0.22 (81)	>30	>30	>30	105	High	100
26m		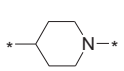	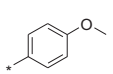	1.01 (71)	NT	NT	NT	127	High	100

(*continued on next page*)

Table 4 (*continued*)

Compd	Amine	Spacer	Ar	Activity[a] EC_{50} μM (E_{max}) α7	Selectivity[a] IC_{50} (μM) α1	α3	5HT3	Sol[b] (μM)	Perm[c]	Met Stab[d]
26n		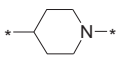	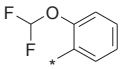	0.24 (77)	>30	>30	>30	124	High	100
26o		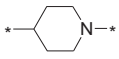	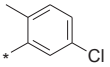	0.24 (94)	>30	19.4	>30	109	High	66
26p		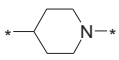	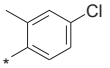	0.24 (76)	>30	>30	>30	98	High	89

[a] Only compounds with α7 activity lower than 1.0 μM were considered suitable for the selectivity evaluation. E_{max} is expressed as percentage of nicotine 10 μM signal. NT indicates not tested.
[b] Solubilities were determined at pH 7.4 at pseudothermodynamic equilibrium.
[c] Permeability is based on measuring the permeation rate of the test article through an artificial membrane. The assay uses a mixture of porcine pig brain lipids in dodecane (2% w/v).
[d] Metabolic stability was determined as percentage remaining after incubation for 1 h with recombinant hCYP3A4.

example compare **21d** with **21c**, **21e** with **21f** and **21g** with **21h**) but none of the examples were completely selective. Also, a positive effect on α7 activity was noted by changing the reference 4-OMe-phenyl ring (see compound **21b**). Groups such as 2-$OCHF_2$-phenyl (**21d** and **21c**), 2-Me-5-Cl-phenyl (**21e** and **21f**) and 2-Me-4-Cl-phenyl (**21g** and **21h**) increased the activity on α7 significantly. All the compounds maintained high solubility and passive permeability as well as good *in vitro* metabolic stability. This SAR exploration showed that the aromatic moieties chosen for Series B were more suitable to increase the activity of our molecules than selectivity. Taking all these results together, we decided to design a small library of hybrid compounds (Series C, Fig. 3A) conjugating the positive effect on selectivity imparted by the cycle-bearing spacer and the amide-pyrazole system known from our previous studies to yield sub-micromolar biological activity. As also suggested by docking studies (Fig. 3B), the hybrid compounds would possess a fixed terminal amino group (pyrrolidine or piperidine), a urea moiety encompassed in a cycle (from Series A) as a spacer, and an amino-pyrazole system (from Series B) to engage the double HBD interaction; four different aryl groups were chosen for a minimal SAR exploration, starting from the most active for Series B.

Results of this library are shown in Table 4 (while an overview of calculated properties is reported in Table S3 of supplementary data). Notably, the combination of the two key moieties of our previous series was successful in terms of both activity and selectivity: most of the compounds showed good activity and complete selectivity for the three related receptors (only compounds **26i** and **26m** had an $EC_{50} > 1$ μM, while **26o** maintained a weak antagonist effect on containing nicotinic α3 receptor with an IC_{50} of 19 μM). As previously observed, 4-OMe-phenyl ring was generally less active than the other aryl rings considered, as demonstrated by compounds **26a**, **26e**, **26i** and **26m**, whose EC_{50} values were higher compared to their direct analogues. Generally very similar activities were observed for the other aryl rings bearing the same amine and spacer. The two different spacers used proved to be equally suitable in terms of activity and selectivity. Interestingly the beneficial effect of pyrrolidine as basic portion of the molecule we noted in series B, was less evident in this series: in most of the compounds comparable activity was observed independently from the amine used (see for example **26b** and **26f**, **26c** and **26g**, **26h** and **26n**, **26k** and **26o**, **26l** and **26p**), while in a few cases piperidine derivatives had lower EC_{50} values than pyrrolidine bearing compounds (**26a** and **26e**, **26d** and **26h**, **26g** and **26m**). All compounds showed good preliminary ADME properties: medium–high solubility at pH 7.4, high passive permeability and good predicted metabolic stability. Almost all the compounds of the library had an optimal preliminary

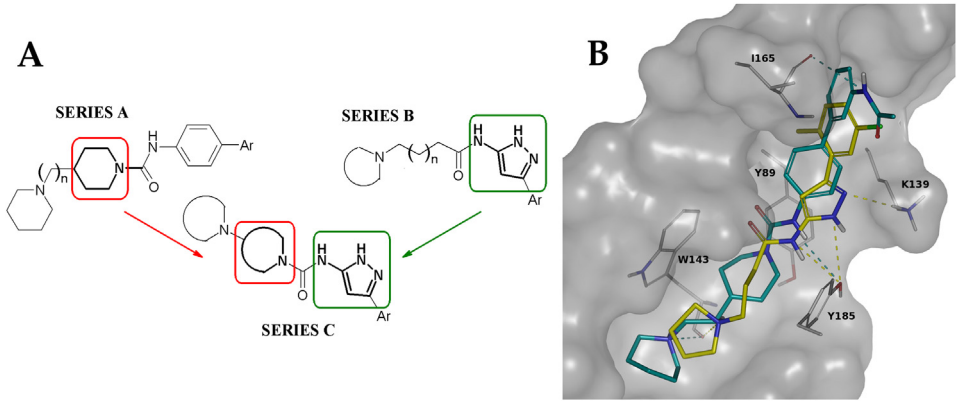

Fig. 3. A. Design of hybrid series C containing the cyclic spacer from series A and the aminopyrazole system from series B. B Compound 16d and 20e bound to the orthosteric site of the theoretical model of human alpha7 nAChR as predicted by molecular docking studies. Residues involved in key interactions are reported. For the sake of clarity, only the binding site is depicted as a surface and part of the Cys-loop has been removed from the image.

in vitro profile, with good activity and excellent selectivity. We chose to characterize **26l**, one of the most promising compounds of the series.

Also in this case the compound showed a very promising profile: no cytochrome (P450 2D6, 3A4 and 2C9) inhibition at 3 μM, medium MDCK permeability and acceptable efflux ratio, excellent *in vitro* intrinsic clearance in human and rat, high plasma stability and good plasma protein binding values in human and rat (Table 5). Pharmacokinetic experiments in rat showed a very good exposure after IP administration (with 96% bioavailability), while moderate exposure and brain to plasma partitioning were observed after PO administration (20% bioavailability and 0.19 B/P). Even if PO data were not optimal, we considered compound **26l** and all Series C analogues a good starting point for further chemistry exploration, considering the good activity levels and the optimal selectivity profile of most of the compounds synthesized.

6. Conclusions

In summary, starting from SAR exploration around our most advanced compounds **1** (very potent but with limited selectivity) and **2** (highly selective but with suboptimal activity values) and supported by docking studies, we designed a hybrid series of molecules which contained the main structural features to achieve good activity values and high selectivity. Using a parallel synthetic approach, we obtained a small library of 16 compounds (**26a**–**p**), most of which fulfilled the activity/selectivity criteria we wanted to achieve and showed an excellent preliminary ADME profile. Despite the moderate oral bioavailability of compound **26l**, this new series of compounds could be a very promising starting point for the design of new molecules aimed at improving the *in vivo* profile.

Table 5
In vitro profiling and pharmacokinetics in rat of compound **26l**.

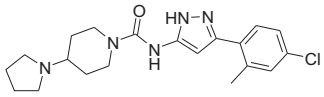

Compound 26l

P450 inhibition[a] **(%)**	**2D6**	−5
	3A4	0
	2C9	7
Permeability	**MDCK P_{app}AB**[b] **(10^{-6} cm/s)**	8.2
	MDCK P_{app}BA/P_{app}AB[c]	3.8
Clint[d] **(μL/min/mg)**	**Hum**	5.0
	Rat	5.0
Plasma stability[e]	**3 h (%)**	113.7
PB[f] **(%)**	**Human**	83.7
	Rat	79.9
PK rat (5 mpk, iv)	**Cl_p**[g] **(mL/min/kg)**	25
	V_{ssh}[g] **(L/Kg)**	7.43
	C_{max} (μM)[g]	0.17
	T_{max} (h)[g]	6
PK rat (5 mpk, po)	**$AUC_{0\text{-}inf}$**[g]	1.7
	F[g]**%**	20
	B/P	0.19
PK rat (5 mpk, ip)	**C_{max} (μM)**[g]	2.10
	T_{max} (h)[g]	0.25
	$AUC_{0\text{-}inf}$[g]	8.1
	F[g]**%**	96.0

[a] Percent cytochrome inhibition values < 15–20% were considered low.
[b] MS-based quantification of apical → basolateral transfer rate of a test compound at 2 μM across contiguous monolayers of MDCK cells.
[c] Ratio of (basal → apical) to (apical → basal) transfer rate of a test compound at 2 μM across contiguous monolayers of MDCK (Madin–Darby canine kidney) cells.
[d] Predicted hepatic clearance from human and rat liver microsomal stability assay.
[e] Plasma stability was determined as percentage remaining after incubation for 3 h with fresh rat plasma.
[f] Protein binding in human and rat plasma expressed as % of the bound compound.
[g] Pharmacokinetic parameters were determined following a single 5 mg/kg dose in male Han Wistar rats. Brain levels were determined following a single 5 mg/kg po dose in male Han Wistar rats, the brain to plasma (B/P) ratio was determined as the ratio of $AUC_{0\text{-}inf}$. See Experimental Section for further details on all assays.

7. Experimental section

7.1. Chemistry

Unless otherwise specified, all nuclear magnetic resonance spectra were recorded using a Varian Mercury Plus 400 MHz spectrometer equipped with a PFG ATB Broadband probe.

^{13}C NMR spectra of several compounds are not completely resolved because the tautomeric equilibrium exchange is slow on the NMR timescale, and the ^{13}C signals of the amino-pyrazole core tend to be very broad. To improve the signal to noise ratio of these specific signals the polarity of the NMR solvent was changed (from DMSO-d6 to CD_3OD, or adding formic acid to free bases DMSO solutions). In case of poor solubility, the experimental temperature (VT) was raised up to 80 °C to enhance the exchange rate between the two tautomeric forms.

HPLC-MS analyses (5 and 10 min methods) were performed with a Waters 2795 separation module equipped with a Waters Micromass ZQ (ES ionization) and Waters PDA 2996, using a Waters XTerra MS C18 3.5 μm, 2.1 × 50 mm column; alternatively, HPLC-MS analyses were performed with an Agilent 1100 instrument, using a Zorbax Eclipse XDB-C8 4.6 × 150 mm; a Zorbax CN 4.6 × 150 mm column or a Zorbax Extend C18 2.1 × 50 mm column, coupled to API-ES MS for the 2.5 min method. Preparative HLPC was run using a Waters 2767 system with a binary Gradient Module Waters 2525 pump and coupled to a Waters Micromass ZQ (ES) or Waters 2487 DAD, using a Supelco Discovery HS C18 5.0 μm, 10 × 21.2 mm column. Gradients were run using 0.1% formic acid/water and 0.1% formic acid/acetonitrile with gradient 5/95 to 95/5 with a runtime of 10 min unless otherwise stated. The purity of compounds submitted for screening were >95% as determined by integrating at 215 nm the peak area of the LC chromatograms. To further support the purity statement, all compounds were also analyzed at a different wavelength (254 nm), and total ion current (TIC) chromatogram and NMR spectra were used to further substantiate results. All column chromatography was performed following the method of Still [28]. All TLC analyses were performed on silica gel (Merck 60 F254) and spots revealed by UV visualization at 254 nm and $KMnO_4$ or ninhydrin stain. All microwave reactions were performed in a CEM Discover oven.

7.2. Synthetic procedures

7.2.1. Synthetic procedures for Route A

Synthesis and characterization of compounds **4**–**6** were previously described [15].

*7.2.1.1. N-{4′-[3-(4-piperidin-1-yl-butyl)-ureido]-biphenyl-3-yl}-acetamide (**7**).* To a degassed solution of **6** (81 mg, 0.23 mmol), 3-acetamido-phenyl boronic acid, (53 mg, 0.3 mmol) was added dissolved in acetonitrile/0.4 N aqueous Na_2CO_3 1/1 (2 mL). After addition of $Pd(PPh_3)_4$ (5–10% mol), the reaction mixture was heated at 90 °C for 20 min under microwave irradiation (power set at 150 W). The acetonitrile layer was separated, the solvent was removed under reduced pressure, and the crude material was purified through an SCX cartridge (eluting with a gradient of DCM/MeOH, followed by MeOH, and finally NH_3/MeOH). The fractions

containing the product were combined and dried under reduced pressure. The title compound was obtained in 43%yield (30 mg). ^{1}H NMR (400 MHz, DMSO-d6) δ 10.04 (s, 1H), 9.77 (s, 1H), 8.93 (s, 1H), 7.81 (s, 1H), 7.53–7.40 (m, 4H), 7.36–7.18 (m, 2H), 6.52 (s, 1H), 3.47–3.27 (m, 2H), 3.12–3.07 (m, 2H), 3.03–2.87 (m, 2H), 2.87–2.70 (m, 2H), 2.04 (s, 3H), 1.81–1.61 (m, 6H), 1.53–1.19 (m, 4H). $C_{24}H_{32}N_4O_2$ Mass (calculated): 408.55; found: 409 [M+1]. HPLC (10 min method); Rt = 2.36; area 98%.

7.2.2. Synthetic procedures for Route B

This route was followed to prepare final compounds **16a–d**.

*7.2.2.1. Synthesis of [1,4′]bipiperidinyl-1′-carboxylic acid (4-bromo-phenyl)-amide (**15a**).* A solution of amine **14a** (3.36 g, 20 mmol) in DCM (40 mL) under nitrogen atmosphere, cooled at 0 °C and then 4-brom-phenyl isocyanate (3.96 g, 20 mmol) was added and the reaction was stirred at 0 °C for 1 h and then allowed to warm up to room temperature and stirred for 1 h. The white precipitate formed was filtered, affording 5.85 g of the desired product **15a** (80% yield). ^{1}H NMR (400 MHz, DMSO-d6) δ 8.58 (s, 1H), 7.45–7.39 (m, 3H), 7.39–7.33 (m, 2H), 4.19–4.04 (m, 2H), 2.71 (t, J = 11.8 Hz, 2H), 2.46–2.31 (m, 5H), 1.76–1.63 (m, 2H), 1.55–1.42 (m, 4H), 1.40–1.15 (m, 4H). $C_{17}H_{24}BrN_3O$ Mass (calculated): 366; found: 366–368 [M+1, Br pattern].

*7.2.2.2. Synthesis of 4-piperidin-1-ylmethyl-piperidine-1-carboxylic acid (4-bromo-phenyl)-amide (**15b**).* To a suspension of N-Boc-isonipecotic acid **8a** (3.0 g, 13.1 mmol) and TBTU (4.2 g, 13.1 mmol) in ACN (60 mL), piperidine (1.67 g, 19.6 mmol) was added. The resulting solution was stirred at 85 °C. for 6 h. The reaction mixture was concentrated under reduced pressure and then dissolved in DCM and washed twice with saturated aqueous Na_2CO_3 solution. Solvent removal gave 3.2 g the 4-(piperidine-1-carbonyl)-piperidine-1-carboxylic acid tert-butyl ester **9a** pure enough for the next stage. **9a** (3.2 g, 10.8 mmol) was dissolved in 25 mL, 6 N HCl solution at 0 °C. After 10 min TLC analysis showed disappearance of starting material, and the mixture was basified to pH 12 with NaOH (pellets) and extracted with AcOEt. The organic phase concentrated under reduced pressure gave 1.9 g of piperidin-4-yl-piperidin-1-yl-methnone (**10a**) that was used without further purification for the next step. **10a** (1.9 g, 9.8 mmol) was added at 0 °C to a suspension of $LiAlH_4$ (0.74 g, 16.7 mmol) in anhydrous THF. After stirring for 30 min the reaction was heated at reflux for 1 h and when TLC analysis showed complete conversion of the starting amide. The reaction was cooled to 0 °C and $LiAlH_4$ was quenched with H_2O and NaOH (10% aqueous solution). The inorganic salts were filtered and the solution was concentrated under reduced pressure, yielding 1.2 g of 4-piperidin-1-ylmethyl-piperidine (**14b**) that was used for the next stage without further purification. To a cooled solution of **14b** (1.2 g, 80% purity, 6.3 mmol) in dichloromethane (20 mL) 4-bromophenylisocyanate (1.24 g, 6.3 mmol) was added and the mixture stirred at 0 °C. until a white solid precipitated out of solution after 2 h. The white solid was filtered off and washed with Et_2O to give 1.2 g of pure title compound **15b** (50% yield). ^{1}H NMR (400 MHz, DMSO-d6) δ 8.54 (s, 1H), 7.44–7.38 (m, 2H), 7.38–7.28 (m, 2H), 4.11–3.99 (m, 2H), 2.80–2.68 (m, 2H), 2.32–2.17 (m, 4H), 2.05 (d, J = 6.8 Hz, 2H), 1.77–1.61 (m, 3H), 1.52–1.40 (m, 4H), 1.40–1.27 (m, 2H), 1.04–0.85 (m, 2H). $C_{18}H_{26}BrN_3O$ Mass (calculated): 380; found: 380-382 [M+1, Br pattern]. HPLC (10 min method); Rt = 2.11; area 99%.

*7.2.2.3. Synthesis of 3-piperidin-1-ylmethyl-piperidine-1-carboxylic acid (4-bromo-phenyl)-amide (**15c**).* To a suspension of N-Boc-nipecotic acid **8b** (3.00 g, 13.1 mmol) and TBTU (4.2 g, 13.1 mmol) in ACN (60 mL), piperidine (2.50 g, 29.4 mmol) was added. The resulting solution was stirred at 85 °C. for 3 h. The reaction mixture was concentrated under reduced pressure and then dissolved in DCM and washed once with saturated aqueous Na_2CO_3 solution and once with 1 N HCl solution. Solvent removal gave 3.8 g the 3-(piperidine-1-carbonyl)-piperidine-1-carboxylic acid tert-butyl ester **9b** pure enough for the next stage. **9b** (3.8 g, 13.1 mmol) was dissolved in 25 mL 6 N HCl solution at 0 °C. After 10 min TLC analysis showed disappearance of starting material, and the mixture was basified to pH 12 with NaOH (pellets) and extracted with AcOEt. The organic phase concentrated under reduced pressure gave 2.03 g of piperidin-3-yl-piperidin-1-yl-methnone (**10b**) that was used without further purification for the next step (yield 78% over 2 steps). **10b** (2.03 g, 10.3 mmol) was added at 0 °C to a suspension of $LiAlH_4$ (0.87 g, 20.7 mmol) in anhydrous THF. After stirring for 30 min the reaction was heated at reflux for 1 h and when TLC analysis showed complete conversion of the starting amide. The reaction was cooled to 0 °C and $LiAlH_4$ was quenched with H_2O and NaOH (10% aqueous solution). The inorganic salts were filtered and the solution was concentrated under reduced pressure, yielding 1.4 g of 4-piperidin-1-ylmethyl-piperidine (**14c**) that was used for the next stage without further purification (yield 74%). To a cooled solution of **14c** (1.4 g, 7.69 mmol) in dichloromethane (20 mL) 4-bromophenylisocyanate (1.45 g, 7.32 mmol) was added and the mixture stirred at 0 °C. until a white solid precipitated out of solution after 2 h. The white solid was filtered off and washed with Et_2O to give 2.1 g of pure title compound **15c** (74% yield). $C_{18}H_{26}BrN_3O$ Mass (calculated): 380; found: 380–382 [M+1, Br pattern]. HPLC (10 min method); Rt = 2.09; area 94%.

*7.2.2.4. Synthesis of 4-(2-piperidin-1-yl-ethyl)-piperidine-1-carboxylic acid (4-bromo-phenyl)-amide (**15d**).* To a solution of 4-(2-hydroxy-ethyl)-piperidine-1-carboxylic acid tert-butyl ester (**11**) in DCM (0.65 mmol/mL) p-toluensulphonyl chloride (1.5 eq) and dimethylaminopyridine (1 eq) were added. The reaction was left at rt for 18 h and then TLC showed complete conversion of the starting material. The mixture was washed with NaOH 2 N and then with HCl 2 N, the organic phase was dried over Na_2SO_4 and then concentrated under reduced pressure. The oil obtained was purified with SiO_2 column, eluting with DCM, giving 4-[2-(Toluene-4-sulfonyloxy)-ethyl]-piperidine-1-carboxylic acid tert-butyl ester (**12**) in quantitative yield. A solution of **12** (4.9 g, 12.8 mmol) in 20 mL of ACN was added to neat piperidine (2.5 mL, 26 mmol) and the reaction was heated at 80 °C for 6 h. When TLC showed complete conversion the mixture was cooled down to room temperature and washed with 20 mL of saturated NaCl water solution. The organic phase was dried over Na_2SO_4 and then concentrated under reduced pressure. The oil obtained was purified by SiO_2 column eluting with 100% DCM to DCM-NH3(2 N MeOH solution)9:1, affording 1.8 g of 4-(2-piperidin-1-yl-ethyl)-piperidine-1-carboxylic acid tert-butyl ester, **13** (yield 46%). To 44 mL of a solution of 6 N HCl, **13** (1.8 g, 6.08 mmol) was added and the reaction was stirred at room temperature for 10 min. The mixture was basified to pH 12 and the product was extracted with 20 mL of DCM. The organic phase was dried over Na_2SO_4 and then concentrated under reduced pressure affording 440 mg of 4-(2-piperidin-1-yl-ethyl)-piperidine **14d** (yield 37%). To a cooled solution of **14d** (440 mg, 2.2 mmol) in dichloromethane (10 mL), 4-bromophenylisocyanate (442 mg, 2.2 mmol) was added and the mixture stirred at 0 °C for 2 h. The mixture was concentrated under reduced pressure and the residue was washed with Et_2O. The solid obtained was filtered giving 750 mg of pure 4-(2-piperidin-1-yl-ethyl)-piperidine-1-carboxylic acid (4-bromo-phenyl)-amide, **15d** (yield 85%). $C_{19}H_{28}BrN_3O$ Mass (calculated) 394; (found): 394–396 [M+1, Br pattern]. HPLC (10 min method); Rt = 2.09; area 92%.

7.2.2.5. General procedure for Suzuki coupling. To a degassed solution of aryl bromide (1 eq), in DME/H_2O (1.8/0.3), the appropriate boronic acid. (1.5 eq) Na_2CO_3 (2 eq), $Pd(OAc)_2$ (10% mol) and tri-o-tolylphosphine (40% mol), were added. The solution was irradiated under microwave conditions for 20 min at power = 200 W. The organic phase was separated and the desired products purified using SCX column and/or prep-HPLC. Fractions containing the desired product were combined and dried under reduced pressure.

*7.2.2.6. [1,4′]Bipiperidinyl-1′-carboxylic acid (3′-acetylamino-biphenyl-4-yl)-amide (**16a**).* Following general procedure of Suzuki Coupling and starting from bromide **15a** and 3-acetamido-phenyl boronic acid, compound 22 mg of **16a** were recovered after SiO_2 column eluting with DCM/TEA (9:1), 18% yield. ^{1}H NMR (400 MHz, CD_3OD) δ 7.79 (d, J = 1.7 Hz, 1H), 7.58–7.39 (m, 5H), 7.39–7.27 (m, 2H), 4.38–4.15 (m, 2H), 2.98–2.79 (m, 2H), 2.72–2.46 (m, 5H), 2.14 (s, 3H), 2.06–1.85 (m, 2H), 1.69–1.59 (m, 4H), 1.58–1.44 (m, 4H). ^{13}C NMR (101 MHz, CD_3OD) δ 170.53, 156.39, 141.54, 139.47, 139.16, 135.46, 129.02, 126.86, 122.16, 121.01, 118.41, 118.08, 62.73, 50.00, 43.73, 27.66, 25.48, 24.17, 22.68. $C_{25}H_{32}N_4O_2$ Mass (calculated) m/z: 420.56; (found): 421 [M+1]. HPLC (10 min method); Rt = 2.11; area 100%.

*7.2.2.7. 4-Piperidin-1-ylmethyl-piperidine-1-carboxylic acid (3′-acetylamino-biphenyl-4-yl)-amide (**16b**).* Following general procedure of Suzuki Coupling and starting from bromide **15b** and 3-acetamido-phenyl boronic acid, 64 mg of **16b** were obtained pure after SCX column (59% yield). ^{1}H NMR (400 MHz, DMSO-d6) δ 9.99 (s, 1H), 8.54 (s, 1H), 7.81 (s, 1H), 7.57–7.39 (m, 5H), 7.36–7.21 (m, 2H), 4.18–4.00 (m, 2H), 2.83–2.63 (m, 2H), 2.26 (s, 4H), 2.13–1.93 (m, 5H), 1.82–1.62 (m, 3H), 1.62–1.31 (m, 6H), 0.98 (d, J = 9.9 Hz, 2H). ^{13}C NMR (101 MHz, CD_3OD) δ 170.52, 156.54, 141.55, 139.57, 139.16, 135.35, 129.04, 126.87, 122.18, 121.04, 118.43, 118.11, 65.38, 54.97, 44.27, 33.37, 31.03, 25.32, 24.12, 22.77. $C_{26}H_{34}N_4O_2$ Mass (calculated): 434.59; (found): 435 [M+1]. HPLC (10 min method); Rt = 2.29; area 100%.

*7.2.2.8. 3-Piperidin-1-ylmethyl-piperidine-1-carboxylic acid (3′-acetylamino-biphenyl-4-yl)-amide (**16c**).* Following general procedure of Suzuki Coupling and starting from bromide **15c** and 3-acetamido-phenyl boronic acid, 28 mg of **16c** were recovered pure after SCX column (28% yield). ^{1}H NMR (400 MHz, CD_3OD) δ 7.79 (s, 1H), 7.53 (d, J = 8.6 Hz, 2H), 7.46 (dd, J = 16.2, 7.8 Hz, 3H), 7.38–7.30 (m, 2H), 4.03–3.96 (m, 1H), 3.90–3.80 (m, 1H), 3.21–3.09 (m, 1H), 2.94–2.82 (m, 1H), 2.62–2.29 (m, 5H), 2.23–2.10 (m, 4H), 1.94–1.78 (m, 2H), 1.80–1.68 (m, 1H), 1.68–1.42 (m, 7H), 1.28 (s, 1H).^{13}C NMR (101 MHz, CD_3OD) δ 170.58, 156.58, 141.53, 139.57, 139.17, 135.45, 129.02, 126.89, 62.02, 54.95, 48.92, 44.88, 33.21, 29.35, 25.43, 25.34, 24.05, 22.69. $C_{26}H_{34}N_4O_2$ Mass (calculated): 434.59; (found): 435 [M+1]. HPLC (10 min method); Rt = 2.38; area 95%.

*7.2.2.9. 4-(2-Piperidin-1-yl-ethyl)-piperidine-1-carboxylic acid (3′-acetylamino-biphenyl-4-yl)-amide (**16d**).* Following general procedure of Suzuki Coupling and starting from bromide **15d** and 3-acetamido-phenyl boronic acid, 65 mg of **16d** were recovered pure after SCX column, followed by preparative HPLC (58% yield). ^{1}H NMR (400 MHz, CD_3OD) δ 7.79 (s, 1H), 7.55–7.50 (m, 2H), 7.48 (dt, J = 7.3, 2.0 Hz, 1H), 7.45–7.40 (m, 2H), 7.37–7.29 (m, 2H), 4.16 (d, J = 13.5 Hz, 2H), 2.97–2.76 (m, 2H), 2.61–2.31 (m, 6H), 2.14 (s, 3H), 1.86–1.73 (m, 2H), 1.70–1.58 (m, 4H), 1.58–1.42 (m, 5H), 1.31–1.15 (m, 3H). ^{13}C NMR (101 MHz, DMSO-d6) δ 169.14, 155.44, 141.15, 141.08, 140.42, 133.80, 129.86, 127.06, 121.57, 120.47, 118.05, 117.36, 112.23, 56.79, 54.82, 44.73, 34.48, 33.75, 32.69, 26.22, 24.86, 24.72. $C_{27}H_{36}N_4O_2$ Mass (calculated):448.61 (found): 449 [M+1]. HPLC (10 min method); Rt = 2.38; area 96%.

*7.2.3. General procedure for 3-Amino-5-aryl pyrazole (**20b–d**)*

To a solution of dry acetonitrile in toluene (1 mmol/mL, 5 eq.) cooled down to −78 °C under nitrogen, a solution of n-butyllithium in n-hexane (1.6 N, 3.5 eq) was added dropwise. The mixture was stirred at −78 °C for 20 min and then a solution of the desired methyl ester (**29b–d**) in toluene (0.75 mmol/mL, 1 eq.) was added and the reaction allowed reaching room temperature. Upon reaction completion, after about 20 min, the mixture was cooled down to 0 °C and HCl 2 N was added to pH 2. The organic phase was recovered, dried over Na_2SO_4 and concentrated under reduced pressure, affording β-ketonitrile (**30b–d**) which was used without further purification. To a solution of the β-ketonitrile (**30b–d**) (7.5 mmoL), in absolute EtOH (15 mL) hydrazine monohydrate (0.44 mL, 9.0 mmol) was added and the reaction was heated at reflux for 18 h. The reaction mixture was allowed to cool to room temperature and the solvent was evaporated under reduced pressure. The residue was dissolved in DCM and washed with water.

The organic phase was concentrated under reduced pressure to give a product that, if not enough pure, was purified by SiO_2 column.

*7.2.3.1. 5-(2-Difluoromethoxy-phenyl)-2H-pyrazol-3-ylamine (**20b**).* Following the general procedure for 3-amino-5-aryl pyrazole synthesis and starting from commercially available 2-difluoromethoxy-benzoic acid methyl ester (**29b**), the title compound was obtained with 76% yield. ^{1}H NMR (400 MHz, DMSO-d6) δ 11.74 (1H, bs), 7.79 (1H, d), 7.00–7.37 (4H, m) 5.79 (1H, s), 4.82 (2H, bs) (d, J = 8.3 Hz, 1H), 7.36–7.32 (m, 1H), 7.29–7.23 (m, 1H), 6.40–6.29 (m, 2H), 5.55 (s, 1H), 2.40 (s, 3H), 1.56 (s, 9H). $C_{21}H_{28}ClN_5O$ Mass (calculated): 225.20; (found): 226 [M+1].

*7.2.3.2. 5-(5-Chloro-2-methyl-phenyl)-2H-pyrazol-3-ylamine (**20c**).* Following the general procedure for 3-amino-5-aryl pyrazole synthesis and starting from 5-chloro-2-methyl-bezoic acid methyl ester (**29c**), the title compound was obtained with 72% yield. ^{1}H NMR (400 MHz, $CDCl_3$) δ 7.34–7.35 (1H, m), 7.22–7.23 (1H, m), 7.19 (1H, bs), 5.78 (1H, s), 3.73 (2H, bs), 2.36 (3H, s). $C_{21}H_{28}ClN_5O$ Mass (calculated): 207.66; (found): 208 [M+1].

*7.2.3.3. 5-(4-Chloro-2-methyl-phenyl)-2H-pyrazol-3-ylamine (**20d**).* Following the general procedure for 3-amino-5-aryl pyrazole synthesis and starting from 4-chloro-2-methyl-bezoic acid methyl ester (**29d**), the title compound was obtained with 62% yield. ^{1}H NMR (400 MHz, $CDCl_3$) δ 7.24–7.26 (2H, m), 7.17–7.20 (1H, m), 5.74 (1H, s), 3.75 (2H, bs), 2.36 (3H, s). $C_{21}H_{28}ClN_5O$ Mass (calculated): 207.66; (found): 208 [M+1].

7.2.4. Synthetic procedures for Route C

This route was followed to prepare final compounds **21c–h** and **22a–b**. Synthesis and characterization of compounds **18a, 18b**, **19a**, **19b**, **21a** and **21b** were previously described [16,17].

*7.2.4.1. General procedure for the synthesis of **21c–h**.* To a suspension of 4-amino-butyric acid **19a** or **19b** (0.75 mmol) in 1,2-dichloroethane (3 mL), N,N′-carbonyldiimidazole (0.75 mmol) was added and the mixture was stirred at room temperature for 2 h (when activation of the aminoacid was complete dissolution of the suspension was generally observed). The desired 3-amino-pyrazole (0.5 mmol) was added. The reaction was stirred for further 10 h. Upon reaction completion (as monitored by LC-MS) if the formation of two isomers was observed, the mixture was heated at 50 °C until the conversion of the less stable isomer to the title compound was

observed (as monitored by LC-MS). The solvent was washed with sat. Na_2CO_3 solution extracted and removed under reduced pressure. The crude products were purified by preparative HPLC.

*7.2.4.2. N-[5-(2-Difluoromethoxy-phenyl)-2H-pyrazol-3-yl]-4-pyrrolidin-1-yl-butyramide, formate salt (**21c**).* Starting from acid **19c** and amino pyrazole **20b**, 101 mg of the desired compound were obtained after preparative HPLC purification (63% yield). ^{1}H NMR (400 MHz, DMSO-d6) δ 10.51 (s, 1H), 8.21 (s, 1H), 7.76 (d, J = 7.6 Hz, 1H), 7.40 (dd, J = 11.0, 4.6 Hz, 1H), 7.34–7.23 (m, 2H), 7.25 (t, J = 73.6 Hz, 1H), 6.87 (s, 1H), 2.70–2.51 (m, 6H), 2.34 (t, J = 7.3 Hz, 2H), 1.82–1.65 (m, 6H). ^{13}C NMR (101 MHz, DMSO-d6, VT = 60 °C) δ 170.53, 165.25, 147.83, 146.63, 139.03, 129.90, 128.99, 125.99, 122.60, 119.60, 119.54, 116.96, 114.39 (t, $^1J_{CF}$ = 258 Hz), 97.22, 54.87, 53.72, 33.55, 23.32, 23.18. $C_{18}H_{22}F_2N_4O_2$ Mass (calculated): 364.40 (found): 365 [M+1]. HPLC (10 min method); Rt = 1.59; area 100%.

*7.2.4.3. N-[5-(2-Difluoromethoxy-phenyl)-2H-pyrazol-3-yl]-4-piperidin-1-yl-butyramide, formate salt (**21d**).* Starting from acid **19a** and aminopyrazole **20b**, 40 mg of the desired compound were obtained after preparative HPLC purification (24% yield). ^{1}H NMR (400 MHz, DMSO-d6) δ 10.53 (s, 1H), 8.23 (s, 1H), 7.77 (dd, J = 7.7, 1.5 Hz, 1H), 7.43–7.37 (m, 1H), 7.35–7.23 (m, 2H), 7.25 (t, J = 73.6 Hz, 1H), 6.87 (s, 1H), 2.59–2.49 (m, 4H), 2.46–2.38 (m, 2H), 2.31 (t, J = 7.3 Hz, 2H), 1.85–1.68 (m, 2H), 1.61–1.48 (m, 4H), 1.39 (d, J = 5.1 Hz, 2H). ^{13}C NMR (101 MHz, DMSO-d6, VT = 80 °C) δ 170.18, 162.92, 147.20, 145.78, 138.50, 128.98, 128.32, 125.17, 122.25, 118.94, 116.26, 96.48, 57.35, 53.43, 33.37, 24.78, 23.42, 21.63. $C_{19}H_{24}F_2N_4O_2$ Mass (calculated): 378.43; (found): 379 [M+1]. HPLC (10 min method); Rt = 1.74; area 100%.

*7.2.4.4. N-[5-(5-Chloro-2-methyl-phenyl)-2H-pyrazol-3-yl]-4-pyrrolidin-1-yl-butyramide, formate salt (**21e**).* Starting from acid **19c** and aminopyrazole **20c**,35 mg of the desired compound were obtained after preparative HPLC purification (42%, yield). ^{1}H NMR (400 MHz, DMSO-d6) δ 12.68 (s, 1H), 10.54 (s, 1H), 8.27–8.14 (m, 1H), 7.47 (t, J = 1.2 Hz, 1H), 7.33 (d, J = 1.4 Hz, 2H), 6.65 (s, 1H), 2.69–2.51 (m, 6H), 2.38–2.30 (m, 5H), 1.83–1.62 (m, 6H). ^{13}C NMR (101 MHz, DMSO-d6, VT = 60 °C) δ 170.09, 164.50, 146.01, 141.48, 134.22, 132.51, 132.14, 130.33, 127.80, 127.60, 96.44, 54.49, 53.15, 33.21, 23.06, 22.89, 19.85. $C_{18}H_{23}ClN_4O$ Mass (calculated): 346.86; (found): 347 [M+1; Cl pattern]. HPLC (10 min method); Rt = 1.84; area 100%.

*7.2.4.5. N-[5-(5-Chloro-2-methyl-phenyl)-2H-pyrazol-3-yl]-4-piperidin-1-yl-butyramide, formate salt (**21f**).* Starting from acid **19a** and aminopyrazole **20c**, 77 mg of the desired compound were obtained after preparative HPLC purification (90%, yield). ^{1}H NMR (400 MHz, DMSO-d6) δ 12.89–11.94 (brs, 1H), 10.40 (s, 1H), 8.15–7.99 (m, 1H), 7.40 (s, 1H), 7.26 (s, 2H), 6.58 (s, 1H), 3.11–2.99 (m, 2H), 2.37–2.16 (m, 9H), 1.65 (s, 2H), 1.43 (s, 4H), 1.29 (s, 2H). ^{13}C NMR (101 MHz, DMSO-d6) δ 170.75, 164.85, 134.90, 133.39, 132.36, 131.10, 128.47, 126.39, 112.55, 97.33, 57.91, 54.02, 33.95, 25.32, 24.04, 22.06, 20.81. $C_{19}H_{25}ClN_4O$ Mass (calculated): 360.89; (found): 361 [M+1; Cl pattern]. HPLC (10 min method); Rt = 1.93; area 100%.

*7.2.4.6. N-[5-(4-Chloro-2-methyl-phenyl)-2H-pyrazol-3-yl]-4-pyrrolidin-1-yl-butyramide (**21g**).* Starting from acid **19c** and aminopyrazole 20d, 16 mg of the desired compound were obtained after preparative HPLC purification (20%, yield). ^{1}H NMR (400 MHz, DMSO-d6) δ 12.52 (s, 1H), 10.43 (s, 1H), 7.49–7.20 (m, 3H), 6.67 (s, 1H), 2.44–2.25 (m, 11H), 1.79–1.54 (m, 6H). ^{13}C NMR (101 MHz, DMSO-d6 + formic acid) δ 169.46, 147.08, 141.05, 138.00, 132.92, 130.63, 130.47, 128.97, 126.23, 96.85, 53.76, 53.48, 32.26, 22.78, 21.43, 20.51. $C_{18}H_{23}ClN_4O$ Mass (calculated): 346.86; (found): 347 [M+1; Cl pattern]. HPLC (10 min method); Rt = 1.88; area 100%.

*7.2.4.7. N-[5-(4-Chloro-2-methyl-phenyl)-2H-pyrazol-3-yl]-4-piperidin-1-yl-butyramide, formate salt (**21h**).* Starting from acid **19a** and aminopyrazole **20d**, 77 mg of the desired compound were obtained after preparative HPLC purification (89%, yield). ^{1}H NMR (400 MHz, DMSO-d6) δ 12.40 (s, 1H), 10.41 (s, 1H), 8.09 (s, 1H), 7.48–7.10 (m, 3H), 6.55 (s, 1H), 2.42–2.19 (m, 11H), 1.78–1.56 (m, 2H), 1.54–1.40 (m, 4H), 1.40–1.20 (m, 2H). ^{13}C NMR (101 MHz, DMSO-d6, VT = 80 °C) δ 170.04, 162.86, 145.84, 141.56, 137.56, 132.30, 130.05, 129.98, 129.20, 125.53, 96.21, 57.04, 53.19, 33.21, 24.36, 23.05, 21.22, 19.89. $C_{19}H_{25}ClN_4O$ Mass (calculated): 360.89; (found): 361 [M+1; Cl pattern]. HPLC (10 min method); Rt = 2.01; area 100%.

7.2.4.8. General procedure of amide reduction. To a solution of amide (0.34 mmol) in anhydrous dioxane (5 mL), 1 M solution of $LiAlH_4$ in THF (0.70 mmol) was added dropwise. The mixture was heated at 80 °C for 1 h. The reaction was allowed to cool down to room temperature and quenched with H_2O and NaOH; inorganic salts were removed by filtration. The solution was concentrated under reduced pressure affording the desired compound pure without further purification.

*7.2.4.9. [5-(4-Methoxy-phenyl)-2H-pyrazol-3-yl]-(5-piperidin-1-yl-pentyl)-amine (**22a**).* Following general procedure of amide reduction and starting from amide **21a**, 23 mg of the desired compound were recovered (20% yield). ^{1}H NMR (400 MHz, DMSO-d6) δ 11.74 (s, 1H), 7.55 (m, 2H), 6.92 (m, 2H), 5.73 (s, 1H), 4.94 (s, 1H), 3.74 (s, 3H), 3.06–2.88 (m, 2H), 2.30–2.21 (m, 4H), 2.22–2.13 (m, 2H), 1.55–1.21 (m, 12H). ^{13}C NMR (101 MHz, DMSO-d6 + FA) δ 158.89, 155.89, 144.49, 126.28, 124.06, 114.20, 86.02, 56.02, 55.25, 52.20, 43.94, 28.90, 23.79, 23.23, 22.74, 21.46. $C_{20}H_{30}N_4O$ Mass (calculated): 342.49; (found): 343 [M+1]. HPLC (10 min method); Rt = 1.31; area 100%.

*7.2.4.10. [5-(4-Methoxy-phenyl)-2H-pyrazol-3-yl]-(4-piperidin-1-yl-butyl)-amine (**22b**).* Following general procedure of amide reduction and starting from amide 21b, 60 mg of the desired compound were recovered (48% yield). ^{1}H NMR (400 MHz, DMSO-d6) δ 11.74 (s, 1H), 7.68–7.39 (m, 2H), 7.06–6.69 (m, 2H), 5.73 (s, 1H), 4.99 (s, 1H), 3.74 (s, 3H), 3.07–2.93 (m, 2H), 2.34–2.14 (m, 6H), 1.55–1.40 (m, 8H), 1.39–1.29 (m, 2H). ^{13}C NMR (101 MHz, DMSO-d6 + formic acid) δ 159.11, 156.02, 144.72, 126.52, 124.05, 114.41, 86.46, 56.10, 55.43, 52.37, 43.79, 26.67, 22.86, 21.61, 21.34. $C_{19}H_{28}N_4O$ Mass (calculated): 328.46; (found): 329 [M+1]. HPLC (10 min method); Rt = 1.19; area 100%.

7.2.5. Synthetic procedures for Route D

This route was followed to prepare final compounds **26a**–**p**.

7.2.5.1. General procedure for Boc protection. Aminopyrazole (2.11 mmol) was dissolved in DCM (10 mL) and a solution of 4.5 M KOH (4.7 mL) was added, followed by di-tert-butylcarbonate (2.11 mmol). The mixture was stirred for 2 days at room temperature and then the organic phase was separated and concentrated under reduced pressure, affording the desired compound pure enough for the next step.

*7.2.5.2. 5-Amino-3-(4-methoxy-phenyl)-pyrazole-1-carboxylic acid tert-butyl ester (**23a**).* following general procedure for Boc protection and starting from 5-amino-3-(4-methoxy-phenyl)-pyrazole (**20a**) 390 mg of **23a** were obtained (64% yield). $C_{15}H_{19}N_3O_3$ Mass (calculated): 289.34; (found): 290 [M+1]. ^{1}H NMR (400 MHz,

DMSO-d6) δ 7.71–7.63 (m, 2H), 6.97–6.92 (m, 2H), 6.34 (d, J = 7.4 Hz, 2H), 5.68 (s, 1H), 3.76 (s, 3H), 1.57 (d, J = 6.6 Hz, 9H).

*7.2.5.3. 5-Amino-3-(2-difluoromethoxy-phenyl)-pyrazole-1-carboxylic acid tert-butyl ester (**23b**).* Following general procedure for Boc protection and starting from 5-amino-3-(2-difluoromethoxy-phenyl)-pyrazole (**20b**) 500 mg of **23b** were obtained (73% yield). ^{1}H NMR (400 MHz, DMSO-d6) δ 7.86 (dd, J = 7.8, 1.8 Hz, 1H), 7.44 (dd, J = 7.6, 1.8 Hz, 1H), 7.29 (td, J = 7.6, 1.1 Hz, 1H), 7.24 (d, J = 6.7 Hz, 1H), 7.23 (t, J = 74.4 Hz, 1H), 6.42–6.30 (m, 2H), 5.79–5.74 (m, 1H), 1.58 (d, J = 6.1 Hz, 9H). $C_{15}H_{17}F_2N_3O_3$ Mass (calculated): 325.32; (found): 326 [M+1].

*7.2.5.4. 5-Amino-3-(5-chloro-2-methyl-phenyl)-pyrazole-1-carboxylic acid tert-butyl ester (**23c**).* Following general procedure for Boc protection and starting from 5-amino-3-(5-chloro-2-methyl-phenyl)-pyrazole **(20c)** 350 mg of **23c** were obtained (54% yield). ^{1}H NMR (400 MHz, DMSO-d6) δ 7.51–7.42 (m, 1H), 7.36–7.24 (m, 2H), 6.42–6.31 (m, 2H), 5.59 (s, 1H), 2.37 (s, 3H), 1.55 (d, J = 2.1 Hz, 9H). $C_{15}H_{18}ClN_3O_2$ Mass (calculated): 307.78; (found): 308 [M+1, Cl pattern].

*7.2.5.5. 5-Amino-3-(4-chloro-2-methyl-phenyl)-pyrazole-1-carboxylic acid tert-butyl ester (**23d**).* Following general procedure for Boc protection and starting from 5-amino-3-(4-chloro-2-methyl-phenyl)-pyrazole (**20d**) 410 mg of **23d** were obtained (63% yield). ^{1}H NMR (400 MHz, DMSO-d6) δ 7.47 (d, J = 8.3 Hz, 1H), 7.36–7.32 (m, 1H), 7.29–7.23 (m, 1H), 6.40–6.29 (m, 2H), 5.55 (s, 1H), 2.40 (s, 3H), 1.56 (s, 9H). $C_{15}H_{18}ClN_3O_2$ Mass (calculated): 307.78; (found): 308 [M+1, Cl pattern].

*7.2.5.6. General procedure for urea synthesis (**26a–d**).* to an aqueous solution of NaOH (1 M, 1.5 eq), a DCM solution of the desired aminopyrazole (**23a–d**) (1 M, 1 eq) was added and the mixture was cooled down to 0 °C. Isopropenyl chloroformate (1.4 eq) was added dropwise and the mixture was allowed to warm up to room temperature. The mixture was stirred for 2 days and then the organic phase was collected and concentrated under reduced pressure, affording the corresponding isopropenyl carbamate (**24a–d**), pure enough for the next step. Isopropenyl carbamate (**24a–d**) (1 eq) was then dissolved in dioxane and the desired amine (**25a–d**) (2 eq). The mixture was heated at 60 °C for 6 h and then solvent was removed under reduced pressure. The residue was dissolved in DCM and trifluoroacetic acid (10 eq) was added and the mixture stirred at room temperature overnight. Solvent was removed under reduced pressure and the residues were purified by preparative HPLC.

*7.2.5.7. [1,3′]Bipyrrolidinyl-1′-carboxylic acid [5-(4-methoxy-phenyl)-2H-pyrazol-3-yl]-amide (**26a**).* Following the general procedure for urea synthesis and starting from aminopyrazole **23a** and amine **25a**, 54 mg of compound **26a** were obtained (68% yield) ^{1}H NMR (400 MHz, DMSO-d6) δ 9.94 (s, 1H), 8.86 (s, 1H), 7.60 (d, J = 8.5 Hz, 2H), 6.97 (d, J = 8.6 Hz, 2H), 6.54 (s, 1H), 3.98–3.82 (m, 1H), 3.81–3.69 (m, 4H), 3.65–3.47 (m, 4H), 3.48–3.29 (m, 1H), 3.13–2.96 (m, 2H), 2.39–2.22 (m, 1H), 2.21–1.95 (m, 3H), 1.94–1.71 (m, 2H). ^{13}C NMR (101 MHz, CD_3OD) δ 160.53, 154.38, 146.77, 146.41, 126.87, 122.32, 114.26, 93.00, 63.32, 54.64, 53.42, 48.53, 43.91, 28.35, 22.96. $C_{19}H_{25}N_5O_2$ Mass (calculated): 355.44; (found): 356 [M+1]. HPLC (10 min method); Rt = 1.26; area 100%.

*7.2.5.8. [1,3′]Bipyrrolidinyl-1′-carboxylic acid [5-(2-difluoromethoxy-phenyl)-2H-pyrazol-3-yl]-amide, formate salt (**26b**).* Following the general procedure for urea synthesis and starting from aminopyrazole **23b** and amine **25a**, 38 mg of compound **26b** were obtained as formate salt after preparative HPLC (44% yield) ^{1}H NMR (400 MHz, DMSO-d6) δ 12.23 (brs, 1H), 8.81 (s, 1H), 8.11 (s, 1H), 7.80 (d, J = 7.9 Hz, 1H), 7.41–7.34 (m, 1H), 7.33–7.25 (m, 2H), 7.24 (t, J = 74.0 Hz, 1H), 6.63 (s, 1H), 3.76–3.60 (m, 1H), 3.59–3.47 (m, 1H), 3.43–3.04 (m, 4H), 2.79 (s, 3H), 2.12 (s, 1H), 1.90 (d, J = 13.4 Hz, 1H), 1.78 (s, 4H). ^{13}C NMR (101 MHz, CD_3OD) δ 160.22, 146.51, 140.01, 138.07, 132.35, 121.26, 120.48, 117.25, 114.36, 110.99, (111.09, 108.52, 105.95), (t, J_{CF} = 259 Hz), 88.74, 55.14, 44.89, 40.24, 35.81, 20.67, 14.66. $C_{19}H_{23}F_2N_5O_2$ Mass (calculated): 391.42; (found): 392 [M+1]. HPLC (10 min method); Rt = 1.41; area 100%.

*7.2.5.9. [1,3′]Bipyrrolidinyl-1′-carboxylic acid [5-(5-chloro-2-methyl-phenyl)-2H-pyrazol-3-yl]-amide (**26c**).* Following the general procedure for urea synthesis and starting from aminopyrazole **23c** and amine **25a**, 37 mg of compound **26c** were obtained as formate salt after preparative HPLC (45% yield). ^{1}H NMR (400 MHz, DMSO-d6) δ 12.16 (s, 1H), 8.83 (s, 1H), 8.11 (d, J = 0.8 Hz, 1H), 7.48 (s, 1H), 7.30 (s, 2H), 6.44 (s, 1H), 3.72–3.60 (m, 1H), 3.59–3.48 (m, 1H), 3.40–3.25 (m, 3H), 2.90–2.71 (m, 4H), 2.35 (s, 3H), 2.21–2.05 (m, 1H), 2.00–1.84 (m, 1H), 1.83–1.70 (m, 4H). ^{13}C NMR (101 MHz, CD_3OD) δ 167.85, 154.75, 146.24, 134.84, 132.57, 132.23, 131.39, 128.39, 128.10, 96.89, 63.45, 53.22, 48.24, 44.09, 28.90, 22.99, 19.14. $C_{19}H_{24}ClN_5O$ Mass (calculated): 373.89; (found): 374 [M+1; Cl pattern]. HPLC (10 min method); Rt = 1.78; area 100%.

*7.2.5.10. [1,3′]Bipyrrolidinyl-1′-carboxylic acid [5-(4-chloro-2-methyl-phenyl)-2H-pyrazol-3-yl]-amide (**26d**).* Following the general procedure for urea synthesis and starting from aminopyrazole **23d** and amine **25a**, 43 mg of compound **26d** were obtained as formate salt after preparative HPLC (52% yield). ^{1}H NMR (400 MHz, DMSO-d6) δ 13.05–10.92 (m, 1H), 8.80 (s, 1H), 8.11 (s, 1H), 7.43 (d, J = 8.3 Hz, 1H), 7.38 (d, J = 2.0 Hz, 1H), 7.30 (dd, J = 8.3, 2.3 Hz, 1H), 6.40 (s, 1H), 3.72–3.59 (m, 1H), 3.57–3.48 (m, 1H), 3.48–3.22 (m, 5H), 2.93–2.67 (m, 4H), 2.36 (s, 3H), 2.18–2.06 (m, 1H), 1.99–1.83 (m, 1H), 1.83–1.69 (m, 4H). ^{13}C NMR (101 MHz, CD_3OD) δ 167.75, 154.77, 146.54, 143.70, 138.33, 133.98, 130.39, 130.28, 129.48, 125.82, 96.96, 63.41, 53.24, 48.30, 44.05, 28.78, 22.99, 19.52. $C_{19}H_{24}ClN_5O$ Mass (calculated): 373.89; (found): 374 [M+1; Cl pattern]. HPLC (10 min method); Rt = 1.71; area 100%.

7.2.5.11. 3-Piperidin-1-yl-pyrrolidine-1-carboxylic acid [5-(4-methoxy-phenyl)-2H-pyrazol-3-yl]-amide (26e). Following the general procedure for urea synthesis and starting from aminopyrazole **23a** and amine **25b**, 68 mg of compound **26e** were obtained (83% yield). ^{1}H NMR (400 MHz, DMSO-d6) δ 12.46 (s, 1H), 9.45 (s, 1H), 8.80 (s, 1H), 7.60 (d, J = 8.5 Hz, 2H), 6.97 (d, J = 8.5 Hz, 2H), 6.54 (s, 1H), 3.80 (s, 1H), 3.76 (s, 3H), 3.61 (t, J = 8.2 Hz, 1H), 3.42 (d, J = 31.0 Hz, 1H), 3.41–3.31 (m, 4H), 3.12–2.71 (m, 2H), 2.37–2.19 (m, 1H), 2.18–1.92 (m, 1H), 1.93–1.19 (m, 6H). ^{13}C NMR (101 MHz, DMSO, VT = 60 °C) δ 159.73, 154.16, 147.41, 144.82, 127.01, 123.58, 114.97, 93.19, 63.64, 55.80, 52.15, 47.22, 44.66, 27.07, 23.20, 21.60. $C_{20}H_{27}N_5O_2$ Mass (calculated): 369.47; (found): 370 [M+1]. HPLC (10 min method); Rt = 1.71; area 100%.

*7.2.5.12. 3-Piperidin-1-yl-pyrrolidine-1-carboxylic acid [5-(2-difluoromethoxy-phenyl)-2H-pyrazol-3-yl]-amide (**26f**).* Following the general procedure for urea synthesis and starting from aminopyrazole **23** and amine **25b**, 61 mg of compound **26f** were obtained (67% yield). ^{1}H NMR (400 MHz, DMSO-d6) δ 12.95–11.90 (m, 1H), 9.13–8.44 (m, 1H), 7.78 (s, 1H), 7.37 (t, J = 7.6 Hz, 1H), 7.33–7.24 (m, 2H), 7.23 (t, J = 74.4 Hz, 1H), 6.89–6.37 (m, 1H), 3.84–3.66 (m, 1H), 3.65–3.48 (m, 1H), 3.29–3.16 (m, 4H), 3.07–2.83 (m, 2H), 2.16 (s, 1H), 1.88 (s, 1H), 1.49 (d, J = 57.7 Hz, 6H). ^{13}C NMR (101 MHz, DMSO-d6) δ 163.90, 153.93, 148.09, 146.83, 139.81, 129.76, 128.87, 126.09, 123.29, 119.66,

117.38 (t, $^1J_{CF}$ = 258.56 Hz), 96.89, 64.30, 52.49, 49.23, 45.19, 28.62, 24.99, 23.57. $C_{20}H_{25}F_2N_5O$ Mass (calculated): 405.45; (found): 406 [M+1]. HPLC (10 min method); Rt = 1.71; area 100%.

*7.2.5.13. 3-Piperidin-1-yl-pyrrolidine-1-carboxylic acid [5-(5-chloro-2-methyl-phenyl)-2H-pyrazol-3-yl]-amide (**26g**).* Following the general procedure for urea synthesis and starting from aminopyrazole **23c** and amine **25b**, 64 mg of compound **26g** were obtained as formate salt after preparative HPLC (75% yield). ^{1}H NMR (400 MHz, DMSO-d6) δ 12.21 (s, 1H), 8.82 (s, 1H), 8.11 (s, 1H), 7.48 (s, 1H), 7.31 (s, 2H), 6.45 (s, 1H), 3.91–3.68 (m, 1H), 3.63–3.48 (m, 1H), 3.40–3.21 (m, 4H), 2.68 (d, *J* = 30.8 Hz, 3H), 2.35 (s, 3H), 2.26–2.07 (m, 1H), 1.98–1.75 (m, 1H), 1.68–1.51 (m, 4H), 1.51–1.33 (m, 2H). ^{13}C NMR (101 MHz, CD_3OD) δ 167.58, 154.64, 146.25, 143.79, 134.83, 132.58, 132.25, 131.38, 128.37, 128.09, 96.86, 64.00, 52.33, 47.29, 44.36, 27.27, 23.43, 21.80, 19.19. $C_{20}H_{26}ClN_5O$ Mass (calculated): 387.92; (found): 388 [M+1; Cl pattern]. HPLC (10 min method); Rt = 1.78; area 100%.

*7.2.5.14. 3-Piperidin-1-yl-pyrrolidine-1-carboxylic acid [5-(4-chloro-2-methyl-phenyl)-2H-pyrazol-3-yl]-amide (**26h**).* Following the general procedure for urea synthesis and starting from aminopyrazole **23d** and amine **25b**, 49 mg of compound **26h** were obtained as formate salt after preparative HPLC (57% yield). ^{1}H NMR (400 MHz, DMSO-d6) δ 12.13 (s, 1H), 8.75 (s, 1H), 8.11 (s, 1H), 7.43 (d, *J* = 8.3 Hz, 1H), 7.40–7.35 (m, 1H), 7.30 (d, *J* = 8.3 Hz, 1H), 6.39 (s, 1H), 3.75–3.64 (m, 1H), 3.59–3.47 (m, 1H), 3.30–3.20 (m, 4H), 3.20–3.06 (m, 4H), 3.06–2.86 (m, 1H), 2.70–2.53 (m, 1H), 2.36 (s, 3H), 2.20–2.02 (m, 1H), 1.83–1.66 (m, 1H), 1.63–1.46 (m, 4H), 1.46–1.28 (m, 2H). ^{13}C NMR (101 MHz, CD_3OD) δ 167.56, 154.74, 146.62, 149.68, 138.34, 133.99, 130.39, 130.29, 129.47, 125.92, 96.98, 64.09, 52.41, 48.24, 44.39, 27.55, 23.72, 20.09, 19.50. $C_{20}H_{26}ClN_5O$ Mass (calculated): 387.92; (found): 388 [M+1; Cl pattern]. HPLC (10 min method); Rt = 1.76; area 100%.

*7.2.5.15. 4-Pyrrolidin-1-yl-piperidine-1-carboxylic acid [5-(4-methoxy-phenyl)-2H-pyrazol-3-yl]-amide, formate salt (**26i**).* Following the general procedure for urea synthesis and starting from aminopyrazole **23a** and amine **25c**, 73 mg of compound **26i** were obtained (89% yield). Mass (calculated) (found): 370 [M+1]. HPLC (10 min method); Rt = 1.36; area 99%. ^{1}H NMR (400 MHz, DMSO-d6) δ 12.78–11.07 (m, 1H), 9.06 (s, 1H), 7.77–7.45 (m, 2H), 7.13–6.87 (m, 2H), 6.51 (s, 1H), 4.29–4.00 (m, 2H), 3.76 (s, 3H), 3.11–2.93 (m, 4H), 2.91–2.83 (m, 1H), 2.83–2.68 (m, 2H), 1.95 (d, *J* = 10.2 Hz, 2H), 1.85 (d, *J* = 29.9 Hz, 4H), 1.57–1.26 (m, 2H). ^{13}C NMR (101 MHz, DMSO-d6, VT = 60 °C) δ 158.89, 154.28, 147.24, 143.32, 126.12, 123.43, 114.18, 92.47, 60.81, 55.09, 50.64, 42.15, 28.83, 22.53.$C_{20}H_{27}N_5O_2$ Mass (calculated): 369.42; (found): 370 [M+1]. HPLC (10 min method); Rt = 1.36; area 99%.

*7.2.5.16. 4-Pyrrolidin-1-yl-piperidine-1-carboxylic acid [5-(2-difluoromethoxy-phenyl)-2H-pyrazol-3-yl]-amide, formate salt (**26j**).* Following the general procedure for urea synthesis and starting from aminopyrazole **23b** and amine **25c**, 73 mg of compound **26j** were obtained as formate salt after preparative HPLC (81% yield). ^{1}H NMR (400 MHz, DMSO-d6) δ 12.04 (bs, 1H), 9.13 (s, 1H), 8.13 (s, 1H), 7.80 (d, *J* = 7.1 Hz, 1H), 7.42–7.35 (m, 1H), 7.33–7.25 (m, 2H), 7.24 (t, *J* = 74.0 Hz, 1H), 6.61 (s, 1H), 4.09 (d, *J* = 13.6 Hz, 2H), 2.96–2.74 (m, 6H), 2.74–2.58 (m, 1H), 2.00–1.84 (m, 2H), 1.83–1.68 (m, 4H), 1.48–1.28 (m, 2H). ^{13}C NMR (101 MHz, DMSO-d6, VT = 60 °C) δ 164.28, 154.39, 147.49, 146.02, 140.00, 129.15, 128.51, 125.50, 119.33, 119.19, 116.62, 114.05, 96.36, 60.83, 50.72, 42.33, 29.43, 22.75. $C_{20}H_{25}F_2N_5O_2$ Mass (calculated): 405.45; (found): 406 [M+1]. HPLC (10 min method); Rt = 1.53; area 100%.

*7.2.5.17. 4-Pyrrolidin-1-yl-piperidine-1-carboxylic acid [5-(5-chloro-2-methyl-phenyl)-2H-pyrazol-3-yl]-amide (**26k**).* Following the general procedure for urea synthesis and starting from aminopyrazole **23c** and amine **25c**, 44 mg of compound **26k** were obtained as formate salt after preparative HPLC (52% yield). ^{1}H NMR (400 MHz, DMSO-d6) δ 12.19 (s, 1H), 9.15 (s, 1H), 8.14 (s, 1H), 7.48 (s, 1H), 7.30 (s, 2H), 6.42 (s, 1H), 4.16–3.97 (m, 2H), 2.91–2.75 (m, 6H), 2.72–2.55 (m, 1H), 2.35 (s, 3H), 1.96–1.82 (m, 2H), 1.82–1.67 (m, 4H), 1.44–1.26 (m, 2H). ^{13}C NMR (101 MHz, CD_3OD) δ 168.73, 155.54, 146.58, 143.87, 134.84, 132.62, 132.23, 131.38, 128.39, 128.09, 96.97.62.12, 51.49, 42.52, 28.71, 22.68, 19.16. $C_{20}H_{26}ClN_5O$ Mass (calculated): 387.92; (found): 388 [M+1; Cl pattern]. HPLC (10 min method); Rt = 1.74; area 100%.

*7.2.5.18. 4-Pyrrolidin-1-yl-piperidine-1-carboxylic acid [5-(4-chloro-2-methyl-phenyl)-2H-pyrazol-3-yl]-amide (**26l**).* Following the general procedure for urea synthesis and starting from aminopyrazole **23d** and amine **25c**, 53 mg of compound **26l** were obtained (62% yield). ^{1}H NMR (400 MHz, DMSO-d6) δ 12.27 (s, 1H), 9.16 (s, 1H), 7.65–7.10 (m, 3H), 6.41 (s, 1H), 4.23–4.08 (m, 2H), 3.24–2.87 (m, 5H), 2.83–2.68 (m, 2H), 2.36 (s, 3H), 2.07–1.90 (m, 2H), 1.91–1.71 (m, 4H), 1.53–1.30 (m, 2H). ^{13}C NMR (101 MHz, CD_3OD + formic acid) δ 163.34, 156.63, 148.09, 144.80, 139.55, 135.28, 131.59, 131.47, 127.13, 98.23, 63.31, 52.82, 43.64, 29.82, 23.83, 20.66. $C_{20}H_{26}ClN_5O$ Mass (calculated): 387.92; (found): 388 (M+1; Cl pattern). HPLC (10 min method); Rt = 1.83; area 100%.

*7.2.5.19. [1,4′]Bipiperidinyl-1′-carboxylic acid [5-(4-methoxy-phenyl)-2H-pyrazol-3-yl]-amide, formate salt (**26m**).* Following the general procedure for urea synthesis and starting from aminopyrazole **23a** and amine **25d**, 63 mg of compound 26m were obtained (74% yield). ^{1}H NMR (400 MHz, DMSO-d6) δ 9.07 (s, 1H), 7.69–7.43 (m, 2H), 7.03–6.88 (m, 2H), 6.51 (s, 1H), 4.23 (d, *J* = 13.7 Hz, 2H), 3.76 (s, 3H), 3.11–2.82 (m, 5H), 2.82–2.68 (m, 2H), 1.90 (d, *J* = 9.7 Hz, 2H), 1.63 (s, 4H), 1.44 (d, *J* = 12.1 Hz, 4H). ^{13}C NMR (101 MHz, CD_3OD) δ 169.73, 161.33, 156.74, 148.64, 146.28, 127.77, 124.31, 115.34, 94.50, 64.96, 55.79, 51.18, 43.95, 27.52, 24.54, 22.97. $C_{21}H_{29}N_5O_2$ Mass (calculated): 383.50; (found): 384 [M+1]. HPLC (10 min method); Rt = 1.49; area 97%.

*7.2.5.20. [1,4′]Bipiperidinyl-1′-carboxylic acid [5-(2-difluoromethoxy-phenyl)-2H-pyrazol-3-yl]-amide (**26n**).* Following the general procedure for urea synthesis and starting from aminopyrazole **23b** and amine **25d**, 47 mg of compound **26n** were obtained as formate salt (50% yield). ^{1}H NMR (400 MHz, DMSO-d6) δ 12.22 (brs, 1H), 9.10 (s, 1H), 8.13 (s, 1H), 7.87–7.61 (m, 1H), 7.38 (t, *J* = 7.9 Hz, 1H), 7.33–7.25 (m, 2H), 7.24 (t, *J* = 73.6 Hz, 1H), 6.60 (s, 1H), 4.27–4.12 (m, 2H), 2.84–2.57 (m, 7H), 1.84–1.70 (m, 2H), 1.61–1.47 (m, 4H), 1.47–1.29 (m, 4H). ^{13}C NMR (101 MHz, CD_3OD) δ 168.72, 155.58, 148.35, 146.71, 140.65, 129.54, 128.78, 125.54, 122.72, 119.31, 116.84 (t, $^1J_{CF}$ = 259.57 Hz), 97.19, 63.75, 49.98, 42.62, 26.37, 23.42, 21.88. $C_{21}H_{27}F_2N_5O_2$ Mass (calculated): 419.48; (found): 420 [M+1]. HPLC (10 min method); Rt = 1.61; area 99%.

*7.2.5.21. [1,4′]Bipiperidinyl-1′-carboxylic acid [5-(5-chloro-2-methyl-phenyl)-2H-pyrazol-3-yl]-amide (**26o**).* Following the general procedure for urea synthesis and starting from aminopyrazole **23c** and amine **25d**, 47 mg of compound **26o** were obtained as formate salt after preparative HPLC (56% yield). ^{1}H NMR (400 MHz, DMSO-d6) δ 11.95 (s, 1H), 9.15 (s, 1H), 8.15 (s, 1H), 7.47 (s, 1H), 7.37–7.22 (m, 2H), 6.42 (s, 1H), 4.25–4.12 (m, 2H), 2.87–2.63 (m, 7H), 2.35 (s, 3H), 1.90–1.74 (m, 2H), 1.64–1.48 (m, 4H), 1.48–1.30 (m, 4H). ^{13}C NMR (101 MHz, CD_3OD) δ 168.63, 155.50, 146.64, 143.68, 134.84, 132.60, 132.23, 131.38, 128.39, 128.09, 96.95, 63.74, 49.97, 42.81, 26.35,

23.38, 21.86, 19.16. $C_{21}H_{28}ClN_5O$ Mass (calculated): 401.94; (found): 402 [M+1; Cl pattern]. HPLC (10 min method); Rt = 1.49; area 97%.

*7.2.5.22. [1,4′]Bipiperidinyl-1′-carboxylic acid [5-(4-chloro-2-methyl-phenyl)-2H-pyrazol-3-yl]-amide (**26p**).* Following the general procedure for urea synthesis and starting from aminopyrazole **23d** and amine **25d**, 44 mg of compound **26p** were obtained as formate salt after preparative HPLC (50% yield). ^{1}H NMR (400 MHz, DMSO-d6) δ 9.10 (s, 1H), 8.14 (s, 1H), 7.43 (d, J = 8.3 Hz, 1H), 7.38 (d, J = 2.0 Hz, 1H), 7.30 (dd, J = 8.3, 2.2 Hz, 1H), 6.38 (s, 1H), 4.26–4.11 (m, 2H), 2.82–2.56 (m, 7H), 2.36 (s, 3H), 1.87–1.71 (m, 2H), 1.62–1.48 (m, 4H), 1.48–1.24 (m, 4H). ^{13}C NMR (101 MHz, CD_3OD) δ 168.67, 155.54, 146.83, 148.74, 138.33, 133.96, 130.39, 130.28, 129.51, 125.92, 97.04, 63.74, 49.97, 42.82, 26.36, 23.40, 21.87, 19.53. $C_{21}H_{28}ClN_5O$ Mass (calculated): 401.94; (found): 402 [M+1; Cl pattern]. HPLC (10 min method); Rt = 1.88; area 100%.

7.3. Biology

7.3.1. Ca^{2+}-flux and membrane potential measurements with a fluorescence imaging plate reader

The following recombinant cell lines were used as specific sources of receptors: GH4C1 cells stably transfected with pCEP4/rat α7 nAChr as previously described [24], HEK293 cell lines stably expressing human 5-HT3A receptors [24]. Native neuroblastoma SH-SY5Y cells were used as source of human ganglionic nAChRs (α3), and TE671 rhabdomyosarcoma cells were used as endogenous source of muscle α1β1δγ receptors. GH4C1 cells expressing α7 and HEK cells expressing 5-HT3A receptors were analyzed by Ca^{2+}-flux measurements employing a Fluorometric Imaging Plate Reader (FLIPR, Molecular Devices) system, whereas the cells expressing the nicotinic receptor subunits α1 and α3 were tested in the FLIPR system with a membrane potential sensitive dye. For Ca^{2+}-flux analysis, cells were plated in 96-well clearbottom, poly D-lysine coated black microtiter plates (Costar) at a density of 1×10^5 cells/well for α7 expressing GH4C1 cells or 8×10^4 cells/well for 5-HT3A expressing HEK293 cells and cultured for 24 h prior to experiments. The medium was then replaced with 100 μL of Hank's Balanced Salt Solution-HEPES 20 mM, pH 7.4 (assay buffer) containing 4 μM Fluo-4-AM, 0.02% pluronic acid, and 5 mM probenecid. After 40 min of incubation at 37 °C, the labeling solution was replaced with 200 μL of assay buffer containing 2.5 mM probenecid. Plates were then transferred to the FLIPR system. Compounds to be tested were prepared in assay buffer as 5x-concentrated solutions in a separate 96-well polypropylene plate. Basal fluorescence was recorded for 30 s, followed by addition of 50 μL of test compound (to assess agonist activity; first addition). Measurements were made at 1 s intervals for 1 min, followed by measurements every 30 s for 10 min. Subsequently, for the second addition for alpha-7 expressing GH4C1 cells, nicotine was added to each well except negative controls at EC_{80} final concentration to assess antagonism of nicotine response or at EC_{20} final concentration to assess positive modulation of nicotine response. Assay performance was robust as reflected by a Z′ factor >0.6. To verify whether the changes in Ca^{+2} levels were specifically due to nAChR opening, we developed a counter screen on GH4C1 wild type cells. The experiment was performed as described above. FPL-64176 1 μM, an L-type Ca^{2+} channel activator, was used a positive control on GH4C1 wt cells. Compounds giving a signal higher than 30% with respect to positive control, at the two highest concentrations, were flagged as unspecific and discarded. For testing 5-HT3A receptor activity, *m*-chlorophenylbiguanide (CPBG, EC80 final concentration) was added to each well except negative controls. Measurements were made at 1 s intervals for 1 min after the second addition and at 3 s intervals for the remaining 3 min. Results were exported from the FLIPR raw data as MAX-MIN of fluorescence signal intensity in two intervals corresponding to the first and the second addition of compounds. The responses were normalized to the positive control and EC_{50} and IC_{50} values were calculated using XlFit version 4.2, with a sigmoidal concentration-response (variable slope) equation: $Y = \text{Bottom} + (\text{Top} - \text{Bottom})/(1 + (EC_{50}/X)^{\text{Hill Slope}})$, where X was the concentration, Y was the response, Bottom was the bottom plateau of the curve, and Top the top plateau. Activity of compounds at the muscle and ganglionic type nAChR receptors was determined using a membrane potential sensitive fluorescent dye. TE671 and SHSY5Y cells were plated at a density of 5×10^4 and 1×10^5 cells/well, respectively, 24 h prior to assay. Growth media were removed from the cells by flicking the plates, and membrane potential dye (Molecular Devices), reconstituted in HBSS five times more diluted compared to the manufacturer's instructions, was added to the wells. Plates were incubated for 60 min at room temperature and then directly transferred to the FLIPR system. Compounds to be tested were prepared in assay buffer as 5×-concentrated solutions in a separate 96-well polypropylene plate. Baseline fluorescence was monitored for the first 10 s followed by the addition of compounds. For detection of antagonist activity, agonist (epibatidine; EC_{80} final concentration) was added to every well except negative controls. Signal recordings were performed as above. Results for SH-SY5Y cells were exported as described previously whereas for TE671 were exported from the FLIPR raw data as SUM of fluorescence signal intensity for the first addition and MAX-MIN for the second addition of compounds. The responses were normalized to the positive control (epibatidine 1 μM final concentration). The compounds tested were found to display antagonist activity, and IC_{50} values were calculated as described before.

7.3.2. Solubility assay

Standard and sample solutions were prepared from a 10 mM DMSO stock solution using an automated dilution procedure. For each compound, three solutions were prepared; one to be used as standard and the other two as test solutions. Standard: 250 μM standard solution in acetonitrile/buffer, with a final DMSO content of 2.5% (v/v). Test sample for pH 3.0: 250 μM sample solution in acetic acid 50 mM, pH = 3, with a final DMSO content of 2.5% (v/v). Test sample for pH 7.4: a 250 μM sample solution in ammonium acetate buffer 50 mM, pH = 7.4, with a final DMSO content of 2.5% (v/v). The 250 μM product suspensions/solutions in the aqueous buffers were prepared directly in Millipore MultiScreen-96 filter plates (0.4 μm PTCE membrane) and sealed. Plates were left for 24 h at room temperature under orbital shaking to achieve "pseudo-thermodynamic equilibrium" and to presaturate the membrane filter. Product suspensions/solutions were then filtered using centrifugation, diluted 1:2 with the same buffer solution, and analyzed by UPLC/UV/TOF-MS, using UV detection at 254 nm for quantitation. Solubility was calculated by comparing the sample and standard UV areas: $S = (A_{smp} \times FD \times C_{st})/A_{st}$, where S was the solubility of the compound (μM), A_{smp} was the UV area of the sample solution, FD was the dilution factor (2), C_{st} was the standard concentration (250 μM), and A_{st} was the UV area of the standard solution.

7.3.3. Cytochrome P450 inhibition assay [29]

The fluorescent P450 inhibition assay was performed using the Gentest method (http://www.gentest.com). Test compounds were dissolved in DMSO at 1.5 mM. The stock solution of 12 μL was added by a robotic system to 1488 μL of 0.1 M phosphate buffer at pH 7.4. The solution was mixed, and 50 μL of the diluted samples was added to a 1 mL 96-well polypropylene plate. Then 50 μL of cofactor with NADPH regenerating system were added to the wells. The

plate was incubated at 37 °C for at 10 min. Enzyme-substrate mix was prepared by prewarming the buffer at 37 °C for at least 10 min, and the enzymes and substrates were added right before addition to the reaction plate. Enzyme-substrate mix (100 μL) was added to the wells to start the reaction. The final substrate and isozyme concentrations and incubation time were: BFC (50 μM)/CYP3A4 (5 pmol/mL) for 30 min, AMMC (1.5 μM)/CYP2D6 (7.5 pmol/mL) for 30 min, and MFC (75 μM)/2C9 (20 pmol/mL) for 45 min. The reactions were stopped with 80% ACN/20% 0.5 M Tris buffer. The signals were quantified using a fluorescent plate reader. The final DMSO concentration was 0.2%. Compounds were tested in duplicates. Percent inhibition was determined at 3 μM compound concentration. High negative values were usually indicative of fluorescent interference from the test compounds or metabolites. The % CV obtained was typically within 10%.

7.3.4. Metabolic stability assay

Compounds in 10 mM DMSO solution were added to an incubation mixture in a 96-well microplate containing 20 pmol/mL of hCYP3A4 (0.1–0.2 mg/mL protein). The mixture was split in two aliquots: one receiving a NADPH regenerating system, the other an equal amount of phosphate buffer. The final substrate concentration was 1 μM along with 0.25% of organic solvent. Incubation proceeded for 1 h at 37 °C and was stopped by addition of acetonitrile to precipitate proteins. Metabolic stability was given as the percent remaining following incubation with cofactor (NADPH) with reference to the incubation mixture without NADPH: % remaining = Area NADPH x 100/Area ctrl where Area ctrl was the MS peak area of the sample solution without NADPH and Area NADPH was the MS area of the sample solution with NADPH. The % CV obtained was typically within 10%.

7.3.5. Permeability assay

The assay was run in a PAMPA filter plate, and compounds (10 μM in HBSS + Hepes buffer pH = 7.4) were added to the donor chamber and incubated for 4 h at 37 °C and 80% humidity. Warfarin was used in each well as control for membrane integrity. Concentrations of reference t(0), donor, and acceptor solutions were measured by UPLC/TOF-MS. The passive permeability was calculated according to the following expression [30]

$$CA(t) = \left(\frac{M}{V_D + V_A}\right) + \left(Ca(0) - \frac{M}{V_D + V_A}\right) e^{-PeA\left(\frac{1}{V_D}+\frac{1}{V_A}\right)t}$$

where M refers to total amount of drug in the system minus the amount of sample lost in membrane (and surfaces), CA(t) was the concentration of the drug in the acceptor well at time t, CA(0) was the concentration of the drug in the acceptor well at time 0, V_A was the volume of the acceptor well, V_D was the volume of the donor well, P_e was the effective permeability, A was the membrane area, and t was the permeation time. Compounds were defined as low, medium, or highly permeable following this classification: $>10 \times 10^{-6}$ cm/s, high (passive permeability was unlikely to be limiting for passive diffusion); between 2 and 10×10^{-6} cm/s, medium (permeability may be limiting in case of low solubility, high metabolic turnover rate or active secretion); between 0 and 2×10^{-6} cm/s, low (high risk that permeability was limiting for passive diffusion).

7.3.6. In vitro intrinsic clearance

Test compounds were incubated separately at 1 μM concentration in 100 mM phosphate buffer (pH 7.4) and 1 mM EDTA with 0.2 mg/mL human or rat hepatic microsomal protein. The enzymatic reaction was initiated by addition of a NADPH regenerating system (final concentrations: 2 mM β-nicotinamide adenine dinucleotide phosphate (NADP) + 10 mM glucose-6-phosphate (G6P) + 0.4 U/ml glucose-6-phosphate dehydrogenase (G6PDH)). Reactions were terminated at regular time intervals (0–5–10–20–40 min) by adding an equal volume of acetonitrile. All incubations were performed in duplicate. Verapamil as positive control for the assay was incubated in parallel under the same conditions. Samples were analyzed by UPLC/TOF-MS. Calculations Substrate depletion data (peak area at different time points) were fitted to a mono-exponential decay model (Eq. (1)), with a 1/y weighting, $C_{(t)} = C_0$ e^{-kt} where C_0 was the substrate concentration in the incubation media at time 0 and k was the terminal rate constant. Under the assumption that the concentration of 1 μM was far below the Km of the test compound, the *in vitro* CL_{int} was calculated by dividing the elimination constant (K) for the microsomal protein concentration (PMS), expressed in mg/μL, to obtain CL_{int} in units of μL/min/mg protein: CL_{int} = K/PMS = μL/min/mg protein. Compounds were defined as low, medium, or highly metabolized based on the *in vitro* CL_{int} values: < 3.4 low, 3.4–92.4 mediun, >92.4 high.

7.3.7. Plasma stability

Fresh plasma spiked with a 250 μM solution of test item dissolved in acetonitrile 12%, were divided in 3 aliquots (one for each time point) in a 96-well plate (in duplicate) and incubated at +37 °C under gentle agitation for up to 3 h. At time 0 and afterwards at the prefixed time points of 30 min and 3 h, two aliquots were transferred and 3 volumes of acetonitrile were added for protein precipitation, followed by centrifugation (4000 rpm, 15 min, 4 °C) and dilution with 0.1% HCOOH. Analysis by LC-ESI$^+$-MSMS using a fast gradient were performed using an API4000 triple quadrupole mass spectrometer (Applied Biosystems) in the multiple reaction monitoring mode (MRM). Results, as average of two replicates, were obtained by comparing the peak area at the different time points (30 min and 3 h) with that at time 0 and were reported as percentage remaining: Percent remaining = Area STM/Area time 0 × 100. Compounds were defined as stable, moderately unstable, or unstable based on the Percent Remaining: 80–100 stable, 50–80 moderately unstable, <50 unstable.

7.3.8. MDCK Cellular permeability

Madin–Darby Canine Kidney were maintained in tissue culture flasks in EMEM with Glutamax added with 1% MEM, Penicillin (100 U/ml), Streptomycin (100 ug/ml), 10% FBS. Five days before the permeability experiment, the cells were split and placed on permeable cell culture inserts (24-well Millipore) at a density of 25,0000 cells/well. Transepithelial electrical resistance (TEER) was measured for each well before incubation using an EVOMX instrument (WPI) to ensure that the monolayer was confluent and the tight junctions intact. A TEER >70 Ohm × cm^2 was considered suitable for experimentation. Compounds (10 μM in HBSS-Hepes buffer) were added in duplicate to the donor chamber and buffer to the acceptor chamber (alternatively apical and basolateral) and incubated for 2 h at 37 °C under gentle agitation. Standards with a high (antipyrin), low (cimetidine) and medium (warfarin) permeability were incubated in the same plate under the same conditions. An aliquot (100 μL) from each well (both apical and basolateral) at time 0 and 120 min was filtered and analysed by UPLC/TOF-MS. Following incubation, the cell monolayer was washed and incubated with Lucifer Yellow, a fluorescent probe with low permeability, to verify monolayer integrity after incubation. The UPLC separation was performed using a C-18 column (Acquity UPLC BEH C18, 1.7 μm, 2.1 × 50 mm, Waters). Samples were analysed using an LTC premier TOF (Waters). The ESI positive W mode scan type was applied and the Total Ion Current (TIC) scan range extended from 100 to 800 amu, with a scan time of 0.08 s. Acquisition was from 0.3 to 1.8 min. Quantitative data were automatically produced using the OpenLynx software. The apparent permeability (P_{app}) in cm/sec

was calculated using the following equation in both directions (apical-to-basolateral and basolateral-to-apical): $P_{app} = dC \times V_r / dt \times A \times C_0$ (where V_r was the volume (mL) of the receiver chamber, A was the surface area of the cell culture insert and dt was the time in sec) Mass balance in both directions was estimated by the following equation: Mass balance = (Final Donor Mass + Mass Transferred)/Initial Donor Mass. The efflux ratio was calculated by comparing $P_{app\ B\to A}$ with $P_{app\ A\to B}$. A high efflux ratio was an indication of the compound being a substrate for efflux transporters. The alert threshold was an efflux ratio >3.

7.3.9. Pharmacokinetics

For i.v. and i.p. administration, compound **26l** was formulated in PEG 400 in saline solution 0.9%/water 50/50 (volume 2.5 mL/kg), while for p.o. administration **26l** was formulated as a solution in 2% Tween, 0.5% methocell in water (volume 2.5 mL/kg). Male HAN Winstar rats (age of 6–8 weeks, body weight 250–550 g) were administered compound **26l** as a single dose of 5 mg/kg (p.o., i.v. and i.p.) at time 0. Levels in plasma were determined over a time period of 24 h in the p.o. and i.p. study and in plasma and brain at 0, 0.5, 1, and 3 h. Concentration of **26l** in rat brain and plasma was measured by high performance liquid chromatography in combination with mass spectrometry (LC-MS/MS) with a limit of detection of 1 ng/mL in plasma and 3 ng/g in brain. Plasma samples were prepared by protein precipitation with acetonitrile containing 250 ng/mL of internal standard centrifugation and analysis of the supernatant by LC-MS/MS. Brain samples were prepared by homogenization and extraction with methanol. The homogenates were subsequently centrifuged, and the supernatant was analyzed by LC-MS/MS. Quantification was performed in a similar manner to the plasma samples.

7.4. Modeling studies

A homology model of the EC domain of nAChR was built by modeling the human α7 sequence for α7 nAChR on 1UW6 PDB structure as a template [11,12] by means of Maestro software suite [31]. Aminoacid numbering reported in the text refers to 1UW6 sequence. The model was then used for docking purposes. Ligands were protonated at pH 7.4 and their geometries optimized using LigPrep module [32]. Docking into the orthosteric binding site of the homology model was performed by the docking program GOLD version 3.0. Ligands were docked using default accurate genetic algorithm settings and the GOLDSCORE fitness function [33]. The goodness of the docked poses was mainly evaluated via visual inspection and supported by the scoring value. Key pharmacophoric interaction between protonated nitrogen on the ligand and the backbone carbonyl of W143 was considered as a fundamental requisite to validate docking poses.

Appendix A. Supplementary data

Supplementary data related to this article can be found at http://dx.doi.org/10.1016/j.ejmech.2014.03.031.

References

[1] J.A. Dani, D. Bertrand, Nicotinic acetylcholine receptors and nicotinic cholinergic mechanisms of the central nervous system, Annual Review of Pharmacology and Toxicology 47 (2007) 699–729.

[2] D. D'hoedt, D. Bertrand, Nicotinic acetylcholine receptors: an overview on drug discovery, Expert Opinion on Therapeutic Targets 4 (2009) 395–411.

[3] C. Gotti, F. Clementi, A. Fornari, A. Gaimarri, S. Guiducci, I. Manfredi, M. Moretti, P. Pedrazzi, L. Pucci, M. Zoli, Structural and functional diversity of native brain neuronal nicotinic receptors, Biochemical Pharmacology 78 (2009) 703–711.

[4] P. Seguela, J. Wadiche, M.K. Dineley, J.A. Dani, J.W. Patrick, Molecular cloning, functional properties, and distribution of rat brain alpha 7: a nicotinic cation channel highly permeable to calcium, Journal of Neuroscience 13 (1993) 596–604.

[5] J. Lindstrom, Neuronal nicotinic acetylcholine receptors, Ion Channels 4 (1996) 377–450.

[6] P. Newhouse, A. Singh, A. Potter, Nicotine and nicotinic receptor involvement in neuropsychiatric disorders, Current Topics in Medicinal Chemistry 4 (2004) 267–282.

[7] C. Gotti, L. Riganti, S. Vailati, F. Clementi, Current Pharmaceutical Design 12 (2006) 407–428.

[8] B.A. Acker, E.J. Jacobsen, B.N. Rogers, D.G. Wishka, S.C. Reitz, D.W. Piotrowski, J.K. Myers, M.L. Wolfe, V.E. Groppi, B.A. Thornburgh, P.M. Tinholt, R.R. Walters, B.A. Olson, L. Fitzgerald, B.A. Staton, T.J. Raub, M. Krause, K.S. Li, W.E. Hoffmann, M. Hajos, R.S. Hurst, D. Walker, Discovery of N-[(3R,5R)-1-azabicyclo[3.2.1]oct-3-yl]furo[2,3-c]pyridine-5-carboxamide as an agonist of the alpha7 nicotinic acetylcholine receptor: in vitro and in vivo activity, Bioorganic & Medicinal Chemistry Letters 18 (2008) 3611–3615.

[9] P. Pichat, O.E. Bergis, J.P. Terranova, A. Urani, C. Duarte, V. Santucci, C. Gueudet, C. Voltz, R. Steinberg, J. Stemmelin, F. Oury-Donat, P. Avenet, G. Griebel, B. Scatton, SSR180711, a novel selective alpha7 nicotinic receptor partial agonist: (II) efficacy in experimental models predictive of activity against cognitive symptoms of schizophrenia, Neuropsychopharmacology 32 (2007) 17–34.

[10] S.N. Haydar, J. Dunlop, Neuronal nicotinic acetylcholine receptors - Targets for the Development of drugs to Treat cognitive Impairment associated with schizophrenia and Alzheimers disease, Current Topics in Medicinal Chemistry 10 (2010) 144–152.

[11] K.R. Tietje, D.J. Anderson, R.S. Bitner, E.A. Blomme, P.J. Brackemeyer, C.A. Briggs, K.E. Browman, D. Bury, P. Curzon, K.U. Drescher, J.M. Frost, R.M. Fryer, G.B. Fox, J. Halvard Gronlien, M. Håkerud, E.J. Gubbins, S. Halm, R. Harris, R.J. Helfrich, K.L. Kohlhaas, D. Law, J. Malysz, K.C. Marsh, R.L. Martin, M.D. Meyer, A.L. Molesky, A.L. Nikkel, S. Otte, L. Pan, P.S. Puttfarcken, R.J. Radek, H.M. Robb, E. Spies, K. Thorin-Hagene, J.F. Waring, H. Ween, H. Xu, M. Gopalakrishnan, W.H. Bunnelle, Preclinical characterization of A-582941: a novel α7 neuronal nicotinic receptor agonist with broad spectrum cognition-enhancing properties, CNS Neuroscience & Therapeutics 14 (2008) 65–82.

[12] A.A. Mazurov, J.D. Speake, D. Yohannes, Discovery and Development of α7 nicotinic acetylcholine receptor modulators, Journal of Medicinal Chemistry 54 (2011) 7943–7961.

[13] J. Malysz, D.J. Anderson, J.H. Grønlien, J. Ji, W.H. Bunnelle, M. Håkerud, K. Thorin-Hagene, H. Ween, R. Helfrich, M. Hu, E. Gubbins, S. Gopalakrishnan, P.S. Puttfarcken, C.A. Briggs, J. Li, M.D. Meyer, T. Dyhring, P.K. Ahring, E.Ø. Nielsen, D. Peters, D.B. Timmermann, M. Gopalakrishnan, In vitro Pharmacological characterization of a novel selective α7 neuronal nicotinic acetylcholine receptor agonist ABT-107, JPET 334 (2010) 863–874.

[14] A.P. Lightfoot, J.N.C. Kew, J. Skidmore, α7 Nicotinic acetylcholine receptor agonists and positive allosteric modulators, Progress in Medicinal Chemistry 46 (2008) 131–171.

[15] C. Ghiron, S.N. Haydar, S. Aschmies, H. Bothmann, C. Castaldo, G. Cocconcelli, T.A. Comery, L. Di, J. Dunlop, T. Lock, A. Kramer, D. Kowal, F. Jow, S. Grauer, B. Harrison, S. La Rosa, L. Maccari, K.L. Marquis, I. Micco, A. Nencini, J. Quinn, A.J. Robichaud, R. Roncarati, C. Scali, G.C. Terstappen, E. Turlizzi, M. Valacchi, M. Varrone, R. Zanaletti, U. Zanelli, Novel alpha-7 nicotinic acetylcholine receptor agonists containing a urea moiety: identification and characterization of the potent, selective, and orally efficacious agonist 1-[6-(4-Fluorophenyl) pyridin-3-yl]-3-(4-piperidin-1-ylbutyl) urea (SEN34625/WYE-103914), Journal of Medicinal Chemistry 53 (2010) 4379–4389.

[16] R. Zanaletti, L. Bettinetti, C. Castaldo, G. Cocconcelli, T. Comery, T.J. Dunlop, G. Gaviraghi, C. Ghiron, S.N. Haydar, F. Jow, L. Maccari, I. Micco, A. Nencini, C. Scali, E. Turlizzi, M. Valacchi, Discovery of a novel Alpha-7 nicotinic acetylcholine receptor agonist series and characterization of the potent, selective, and orally efficacious agonist 5-(4-Acetyl[1,4]diazepan-1-yl)pentanoic acid [5-(4-Methoxyphenyl)-1H-pyrazol-3-yl] amide (SEN15924, WAY-361789), Journal of Medicinal Chemistry 10 (2012) 4806–4823.

[17] R. Zanaletti, L. Bettinetti, C. Castaldo, I. Ceccarelli, G. Cocconcelli, T.A. Comery, J. Dunlop, E. Genesio, C. Ghiron, S.N. Haydar, F. Jow, L. Maccari, I. Micco, A. Nencini, C. Pratelli, C. Scali, E. Turlizzi, M. Valacchi, N-[5-(5-Fluoropyridin-3-yl)-1H-pyrazol-3-yl]-4-piperidin-1-ylbutyramide (SEN78702, WYE-308775): a medicinal chemistry effort toward an α7 nicotinic acetylcholine receptor agonist Preclinical candidate, Journal of Medicinal Chemistry 22 (2012) 10277–10281.

[18] W. Seelen, M. Schafer, A. Ernst, Selective ring N-protection of aminopyrazoles, Tetrahedron Letters 44 (2003) 4491–4493.

[19] I. Gallou, M. Eriksson, X. Zeng, C. Senanayake, V.J. Farina, Practical synthesis of unsymmetrical ureas from isopropenyl carbamates, Journal of Organic Chemistry 70 (2005) 6960–6963.

[20] P. Seneci, M. Nicola, M. Inglesi, E. Vanotti, G. Resnati, G, Synthesis of mono- and disubstituted 1H-imidazo [1,2-B] pyrazoles, Synthetic Communications 29 (1999) 311–341.

[21] S.D. Larsen, C.H. Spilman, H. Charles, F.P. Bell, D.M. Dinh, E. Martinborough, G.J. Wilson, Synthesis and hypocholesterolemic activity of 6,7-dihydro-4H-pyrazolo[1,5-a]pyrrolo[3,4-d]pyrimidine-5,8-diones, novel inhibitors of acyl-CoA: cholesterol O-acyltransferase, Journal of Medicinal Chemistry 34 (1991) 1721–1727.

[22] N. Suryakiran, T. Srikanth Reddy, K. Asha Latha, P. Prabhakar, K. Yadagiri, Y. Venkateswarlu, An expeditious synthesis of 3-amino 2H-

pyrazoles promoted by methanesulphonic acid under solvent and solvent free conditions, Journal of Molecular Catalysis A: Chemical 258 (2006) 371–375.
[23] J.Q. Puello, B.I. Obando, C. Foces-Foces, L. Infantes, R.M. Claramunt, P. Cabildo, J.A. Jimenez, J. Elguero, Structure and tautomerism of 3(5)-Amino-5(3)-arylpyrazoles in the solid state and solution: an X-ray and NMR study, Tetrahedron 53 (31) (1997) 10783–10802.
[24] J. Dunlop, R. Roncarati, B. Jow, H. Bothmann, T. Lock, D. Kowal, M. Bowlby, G.C. Terstappen, *In vitro* screening strategies for nicotinic receptor ligands, Biochemical Pharmacology 74 (2007) 1172–1181.
[25] R.L. Papke, J.K. Porter Papke, Comparative pharmacology of rat and human a7 nAChR conducted with net charge analysis, British Journal of Pharmacology 137 (2002) 49–61.
[26] D.F. Veber, S.R. Johnson, H.Y. Cheng, B.R. Smith, K.W. Ward, K.D. Kopple, Molecular properties that influence the oral bioavailability of drug candidates, Journal of Medicinal Chemistry 45 (2002) 2615–2623.
[27] P.R. Andrews, D.J. Craik, J.L. Martin, Functional group contributions to drug-receptor interactions, Journal of Medicinal Chemistry 27 (1984) 1648–1657.
[28] W.C. Still, M. Kahn, A. Mitra, Rapid chromatographic technique for preparative separations with moderate resolution, Journal of Organic Chemistry 14 (1978) 2923–2925.
[29] C.L. Crespi, V.P. Miller, B.W. Penman, Microtiter plate assays for inhibition of human, drug-metabolizing cytochromes P450, Analytical Biochemistry 248 (1997) 188–190.
[30] K. Palm, K. Luthman, J. Ros, J. Gråsjö, P. Artursson, Effect of molecular charge on intestinal epithelial drug transport: ph-dependent transport of cationic drugs, Journal of Pharmacology and Experimental Therapeutics 291 (1999) 435–443.
[31] Maestro, Version 9.0, Schrodinger, LLC, New York, NY, 2010.
[32] LigPrep, Version 2.3, SchrOdinger, LLC, New York, NY, 2010.
[33] G. Jones, P. Willett, R.C. Glen, A.R. Leach, R. Taylor, Development and Validation of a genetic algorithm for Flexible docking, Journal of Molecular Biology 267 (1997) 727–748.